Pulmonary Pharmacology & Therapeutics 22 (2009) 487–491

Contents lists available at ScienceDirect

Pulmonary Pharmacology & Therapeutics

journal homepage: www.elsevier.com/locate/ypupt

N-acetyl-L-cysteine inhibits TGF-β_1-induced profibrotic responses in fibroblasts

Hisatoshi Sugiura [a,*], Tomohiro Ichikawa [a], Xiangde Liu [b], Tetsu Kobayashi [b], Xing Qi Wang [b], Shin Kawasaki [b], Shinsaku Togo [b], Koichiro Kamio [b], Lijun Mao [b], Youngsoo Ann [b], Masakazu Ichinose [a], Stephen I. Rennard [b]

[a] Third Department of Internal Medicine, Wakayama Medical University School of Medicine, 811-1 Kimiidera, Wakayama, Wakayama 641-0012, Japan
[b] University of Nebraska Medical Center, 985885 Nebraska Medical Center, Omaha, NE 68198-5885, USA

ARTICLE INFO

Article history:
Received 5 September 2008
Received in revised form
22 December 2008
Accepted 14 April 2009

Keywords:
Collagen gel contraction
Myofibroblast
Fibronectin
Vascular endothelial growth factor

ABSTRACT

Background: Excessive production of TGF-β_1 plays a key role in the tissue remodeling or fibrotic process observed in bronchial asthma, chronic pulmonary disease (COPD), and idiopathic pulmonary fibrosis (IPF). TGF-β_1 has been reported to decrease the intracellular glutathione level and stimulate the production of reactive oxygen species.

Objectives: The aim of this study was to evaluate whether the antioxidant N-acetyl-L-cysteine (NAC) can affect TGF-β_1-mediated tissue remodeling in fibroblasts or modulate the production of fibronectin and vascular endothelial growth factor (VEGF) which are believed to be important mediators of tissue repair and remodeling.

Methods: To accomplish this, human fetal lung fibroblasts (HFL-1) were used to assess the effect of NAC on the TGF-β_1-mediated contraction of floating gels and the TGF-β_1-induced mediator production. In addition, the effect of NAC on the TGF-β_1-induced differentiation to myofibroblasts was evaluated by assessing α-smooth muscle actin (α-SMA) expression.

Results: NAC significantly abolished the TGF-β_1-augmented gel contraction (at 3 mM, gel size $63.4 \pm 2.6\%$ vs. $39.1 \pm 4.1\%$; $p < 0.01$) compared with control in a concentration-dependent manner. NAC also significantly inhibited the TGF-β_1-augmented fibronectin ($p < 0.01$) and VEGF ($p < 0.01$) production in the media of both the three-dimensional gel and monolayer culture. Furthermore, NAC reversed the TGF-β_1-stimulated α-SMA expression ($p < 0.01$).

Conclusion: These results suggest that NAC can affect the TGF-β_1-induced tissue remodeling or fibrotic process in vitro.

1. Introduction

Fibroblasts play a pivotal role in the normal wound healing or tissue repair process [1], whereas excessive stimuli for fibroblasts lead to the tissue remodeling or fibrous tissue that is observed in bronchial asthma [2], chronic obstructive pulmonary disease (COPD) [3] and idiopathic lung fibrosis (IPF) [4].

Transforming growth factor (TGF)-β_1 is a multifunctional cytokine in a variety of physiological and pathological processes, including fibroblast repair responses [5,6]. TGF-β_1 regulates the fibroblast migration, proliferation, differentiation and production of matrix. In addition, TGF-β_1 stimulates the fibroblast-mediated contraction of extracellular matrix [7].

N-acetylcysteine (NAC) is a non-toxic aminothiol that has a strong reductive capacity [8]. Because NAC is not only a precursor of GSH but also shows a direct ROS-scavenging capacity, NAC has been widely used as a potent antioxidant. In cultured fibroblasts, NAC inhibited the TGF-β_1-stimulated collagen production [9]. Moreover, aerosolized administration of NAC attenuates the lung fibrosis induced by bleomycin in mice [10]. These results suggest that antioxidant may suppress TGF-β_1 signaling in vitro and in vivo.

Recently, Meurer et al. clearly showed that NAC itself reduced the disulfide bonds of TGF-β_1 and changed the bioactive form (dimmer) to the inactive form (monomer) [11]. Moreover, NAC changed the binding activity of TGF-β_1 to its receptor in hepatic stellate cells [11], suggesting that the effect of antioxidant NAC is based on a direct blockade of TGF-β_1 function and signaling. However, it has not been fully elucidated whether NAC can modulate the TGF-β_1-induced tissue repair, mediator production and differentiation in human lung fibroblasts.

In the current study, we used a fibroblast-mediated collagen gel contraction assay as a tissue repair model in the current study and assessed the effect of NAC on the TGF-β_1-stimulated collagen gel contraction. We investigated whether NAC affected the production of

* Corresponding author. Tel.: +81 73 441 0619; fax: +81 73 446 2877.
E-mail address: sugiura@wakayama-med.ac.jp (H. Sugiura).

1094-5539/$ - see front matter © 2009 Elsevier Ltd. All rights reserved.
doi:10.1016/j.pupt.2009.04.002

fibronectin and vascular endothelial growth factor (VEGF), which are believed to be important mediators of repair and remodeling. Furthermore, we evaluated the effect of NAC on the TGF-β-induced differentiation to myofibroblasts by assessing α-smooth muscle actin (α-SMA) expression.

2. Materials and methods

2.1. Materials

Native type I collagen [rat tail tendon collagen (RTTC)] was extracted from rat tail tendons by a previously published method [12]. Briefly, tendons were excised from rat tails, and the tendon sheath and other connective tissues were removed carefully. Repeated washing with Tris-buffered saline (0.9% NaCl and 10 mM Tris, pH 7.5) was followed by dehydration and sterilization with 50%, 75%, 95% and pure ethanol. Type I collagen was then extracted in 6 mM hydrochloric acid at 4 °C. The collagen concentration was determined by weighing a lyophilized aliquot from each lot of collagen solution. Sodium dodecylsulfate-polyacrylamide gel electrophoresis (SDS-PAGE) consistently demonstrated no detectable proteins other than type I collagen.

Commercially available reagents were obtained as follows: TGF-β_1 was from R&D Systems (Minneapolis, MN); N-acetylcysteine (NAC), 3,3′,5,5′-tetramethyl benzidine (TMB), monoclonal anti-human fibronectin antibody, and polyclonal anti-human fibronectin antibody were purchased from Sigma (St. Louis, MO); Dulbecco's Modified Eagle's Medium (DMEM) and fetal calf serum (FCS) were from Invitrogen Life Technologies (Grand Island, NY).

2.2. Cell culture

Human fetal lung fibroblast (HFL-1) cells were obtained from the American Type Culture Collection (Rockville, MD). The cells were cultured on tissue culture dishes (Falcon; Becton–Dickinson Labware, Lincoln Park, NJ) with DMEM supplemented with 10% FCS, 100 mg/ml penicillin, 250 μg/ml streptomycin and 2.5 μg/ml fungizone. The cells were cultured at 37 °C in a humidified atmosphere of 5% CO_2 and passaged every 4–5 days at a 1:4 ratio. HFL-1 cells were used between the 14th and 18th passages. To evaluate mediator production in a monolayer culture, the cells were seeded in 6-well tissue culture plates at a cell density of 1×10^5/ml. At 90% confluence, the cells were treated with various concentrations of NAC in serum-free DMEM (SF-DMEM) in the presence or absence of TGF-β_1. The supernatants of the monolayer culture were harvested on day 3 and stored at −80 °C until later assay.

2.3. Western blotting

Immunoblotting of α-SMA was performed. To detect α-SMA, the cells were seeded in 60 mm dishes at a density of 1×10^5 cell/ml and cultured for 24 h, and then the medium was replaced with SF-DMEM for 24 h. The cells were pretreated with or without NAC for 2 h and then further treated with vehicle or TGF-β_1 for 48 h. The cells were then harvested and homogenized in cell lysis buffer. All samples were eluted at 97 °C for 5 min in sodium dodecylsulfate (SDS)-PAGE sample buffer. Five milligrams of whole cell lysate for α-SMA was separated by electrophoresis on 12% SDS polyacrylamide gels. After electrophoresis, the separated proteins were transferred to a PVDF membrane (Bio-Rad Laboratories, Hercules, CA). The membrane was incubated with mouse monoclonal anti-α-SMA antibody (1:5000 dilution; Sigma, St. Lois, MO) at 4 °C overnight. Bound antibody was visualized using peroxidase-conjugate anti-mouse IgG antibody and enhanced chemiluminescence (Amersham Biosciences, Buckinghamshire, UK) with Typhoon Scanner (Amersham Biosciences). Densitometry was used to quantify the expression of α-SMA by using NIH image.

2.4. Collagen gel contraction assay

Collagen gels were prepared as described previously [13]. Briefly, RTTC, distilled water and 4× concentrated DMEM were combined so that the final mixture resulted in 0.75 mg/ml collagen, with a physiological ionic strength of 1× DMEM and a pH 7.4. The cells were trypsinized (trypsin–EDTA; 0.05% trypsin, 0.53 mM EDTA-4Na, GIBCO) and suspended in SF-DMEM. The cells were then mixed with the neutralized collagen solution so that the final cell density in the collagen solution was 3×10^5 cells/ml, and the final concentration of collagen was 0.75 mg/ml. Aliquots (0.5 ml/well) of the mixture of cells in collagen were cast into each well of 24-well tissue culture plates (Falcon) and allowed to gel. After gelation was completed, normally within 20 min at room temperature, the gels were gently released from the 24-well tissue culture plates and transferred into 60 mm tissue culture dishes (three gels in each dish), which contained 5 ml of freshly prepared 0.2% FCS containing DMEM with or without various concentrations of NAC in the presence or absence of TGF-β_1. The gels were then incubated at 37 °C in a 5% CO_2 atmosphere for 3 days. Gel size was measured using an Optomax V image analyzer (Optomax, Burlington, MA) daily. Data were expressed as percentages of the original gel size.

2.5. Measurement of fibronectin and VEGF by ELISA

Soluble form of fibronectin and VEGF in the media of the collagen gel culture or monolayer culture was determined by ELISA. Quantification of fibronectin was performed as previously described [14]. Briefly, plates were coated with monoclonal anti-fibronectin antibody (1:10000 dilution) at 4 °C overnight. After being washed three times, standards and samples were added and incubated at room temperature for 2 h. After being washed, bound antigen was detected after adding polyclonal anti-human fibronectin antibody (1:2500 dilution) at room temperature for 1 h. After being washed, HRP conjugated anti-rabbit IgG antibody (1:2500 dilution; Rockland, Gilbertsville, PA) was added at room temperature for 1 h. After being washed, bound HRP was detected with 0.1 mg/ml OPD. The reaction was stopped with 8 M H_2SO_4, and the product was quantified at 490 nm with a microreader. Quantification of VEGF was performed as follows. Plates were coated with 50 ng/ml monoclonal anti-human VEGF antibody (R&D system, Minneapolis, MN) at 4 °C overnight. After being washed three times, standards and samples were added and incubated at room temperature for 2 h. After being washed, bound antigen was detected after adding 100 ng/ml biotinylated-anti-human VEGF antibody (R&D system, Minneapolis, MN) for 1 h at room temperature. After being washed, HRP–streptavidin (1:20000 dilution; Zymed Laboratories, San Francisco, CA) was then added for 1 h. Bound HRP was detected with TMB. The reaction was stopped with 1 M H_2SO_4, and the product was quantified at 450 nm with a microreader.

2.6. Statistical analysis

Data were expressed as means ± SEM. Experiments with multiple comparisons were evaluated by one way analysis of variance (ANOVA) followed by Bonferroni's test to adjust for multiple comparisons. Probability values of less than 0.05 were considered significant.

3. Results

3.1. Effect of NAC on the TGF-β_1-augmented collagen gel contraction mediated by fibroblasts

To evaluate whether NAC can affect the TGF-β_1-induced tissue repair process, we assessed the effect of NAC by using a collagen gel contraction assay. The cells were pretreated with various

concentrations of NAC for 2 h prior to treatment with TGF-β_1. TGF-β_1 significantly augmented the three-dimensional (3D) collagen gel contraction compared with control on day 3 (at 100 pM, gel size was 39.1 ± 4.1% vs. 61.9 ± 1.1% of initial size; $p < 0.01$, Fig. 1A, B). NAC (0.3–3 mM) significantly blocked the TGF-β_1-augmented collagen gel contraction on day 3 in a concentration-dependent manner (at 3 mM, gel size was 63.4 ± 2.6% vs. 39.1 ± 4.1%; $p < 0.01$, Fig. 1A, B).

3.2. Effect of NAC on fibronectin and VEGF release by fibroblasts in the media of collagen gels and monolayer culture

To evaluate the effect of NAC on fibronectin production, the fibronectin level in the media of the collagen gel and monolayer cultures was measured by ELISA. TGF-β_1 significantly increased fibronectin release in both the 3D gel ($p < 0.01$, Fig. 2A, left panel) and monolayer culture ($p < 0.01$, Fig. 2A, right panel). NAC significantly blocked TGB-β_1-augmented fibronectin release in a concentration-dependent manner in both the 3D gel ($p < 0.01$, Fig. 2A, left panel) and monolayer culture ($p < 0.01$, Fig. 2A, right panel).

We also assessed the effect of NAC on VEGF production by fibroblasts. As shown in Fig. 2B, TGF-β_1 significantly increased VEGF release in both the 3D gel ($p < 0.01$, Fig. 2B, left panel) and monolayer culture ($p < 0.01$, Fig. 2B, right panel), whereas NAC significantly blocked the TGF-β_1-augmented VEGF release in both the 3D gel ($p < 0.01$, Fig. 2B, left panel) and monolayer culture ($p < 0.01$, Fig. 2B, right panel).

3.3. Effect of NAC on the TGF-β_1-augmented expression of α-SMA

To evaluate whether NAC affects the differentiation to myofibroblasts, we investigated the effect of NAC on the expression of α-SMA, which is a marker of differentiation to myofibroblasts. TGF-β_1 significantly stimulated α-SMA expression in the fibroblasts ($p < 0.01$, Fig. 3A, B). Ten mM NAC abolished the TGF-β_1-stimulated expression of α-SMA ($p < 0.01$, Fig. 3A, B), suggesting that NAC could inhibit the TGF-β_1-stimulated differentiation to myofibroblasts.

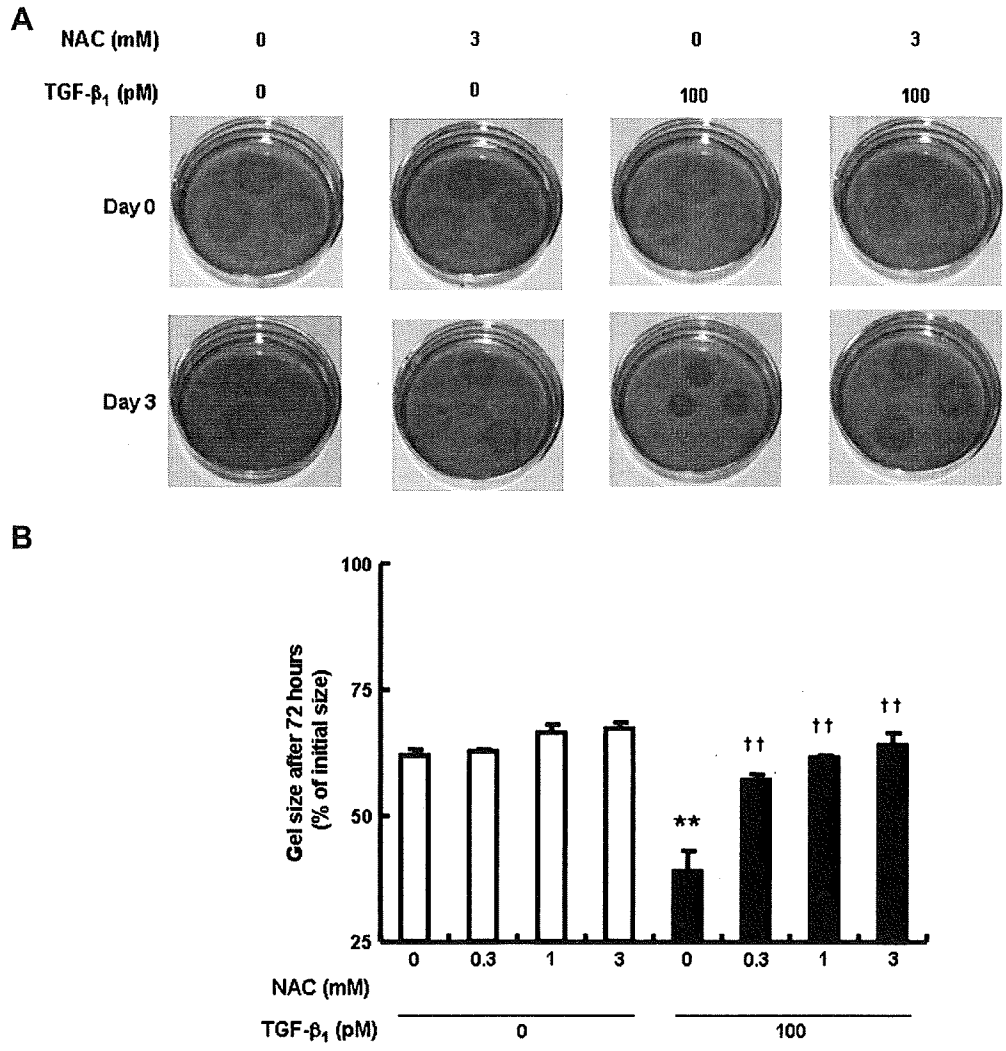

Fig. 1. Effect of NAC on collagen gel contraction mediated by human fibroblasts. Fibroblasts were cast into three-dimensional collagen gels and floated in medium containing various concentrations of NAC for 2 h prior to treatment with TGF-β_1. Gel size was measured daily. Representative photographs of collagen gel contraction assay are presented (Panel A). Gel size after 72 h is presented (Panel B). Panel B: vertical axis: gel size after 72 h incubation (% of initial size); horizontal axis: NAC concentration (mM) and TGF-β_1 concentration (pM). All values are mean ± SEM for three separate experiments, each performed in triplicate. $^{**}p < 0.01$; compared with the values of control. $++p < 0.01$; compared with the values of TGF-β_1 treated group.

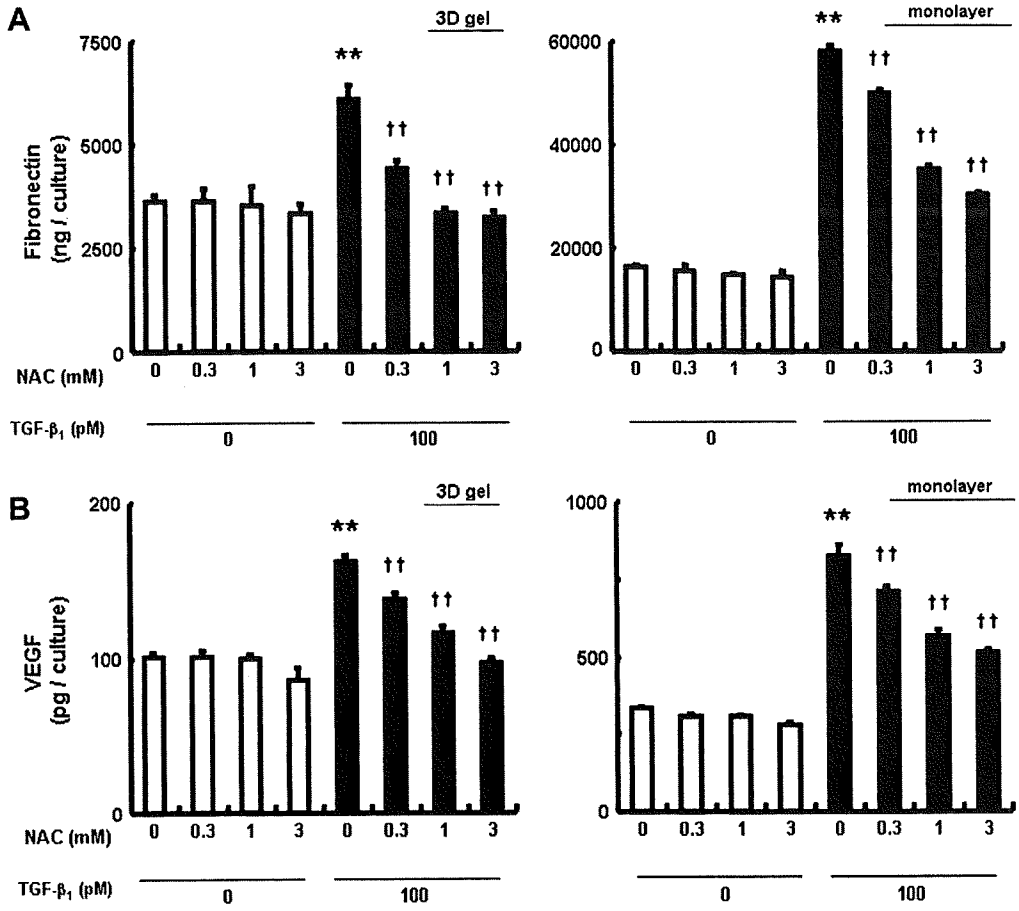

Fig. 2. Effect of NAC on the TGF-β_1-augmented fibronectin release (Panel A) and vascular endothelial growth factor (VEGF) (Panel B) in the culture media. Fibroblasts were cast into collagen gels and maintained in floating culture in medium in the presence of varying concentrations of NAC. After 2 h, gels were treated with or without TGF-β_1 (left panels). In a separate experiment, fibroblasts were cultured until 90% confluence, after which the medium was changed to serum-free DMEM with varying concentrations of NAC. After treatment with or without NAC, the cells were further treated with or without TGF-β_1 (right panels). After 3 days, media were harvested and assayed for fibronectin (A) or VEGF (B) by ELISA. Vertical axes: fibronectin (ng/culture) or VEGF production (pg/culture); horizontal axes: NAC concentration (mM) and TGF-β_1 concentration (pM). All values are mean ± SEM for five separate experiments, each performed in duplicate. $^{**}p < 0.01$; compared with the values of control. $^{++}p < 0.01$; compared with the values of TGF-β_1 treated group.

4. Discussion

The present study demonstrated that NAC inhibited the TGF-β_1-augmented collagen gel contraction, mediator production and α-SMA expression. These results suggest that NAC can affect the tissue repair process in vitro.

NAC is a non-toxic aminothiol, a potent antioxidant, and a synthetic precursor of GSH. NAC is frequently used as an antioxidant in in vitro and in vivo studies. A previous report showed that NAC reduced the intracellular GSH level and production of reactive oxygen species (ROS) [15]. NAC was also reported to inhibit TGF-β_1-stimulated collagen production [9]. These results suggested that intracellular ROS produced by TGF-β_1 was related to TGF-β_1-induced phenomena. Recently, Meurer et al. showed that NAC not only changed TGF-β_1 to the biologically inactive form but also inhibited the binding of TGF-β_1 to its receptor [11]. On the basis of this study, we investigated whether NAC can inhibit TGF-β_1-augmented collagen gel contraction, which is a model of wound healing and tissue remodeling. As shown in Fig. 1, NAC significantly inhibited the TGF-β_1-augmented collagen gel contraction. We also investigated the TGF-β_1-augmented production of fibronectin and VEGF because these mediators were reported to have important roles in wound healing and tissue remodeling [16,17]. NAC inhibited the TGF-β_1-augmented mediator release in the media of both the collagen gel and monolayer culture. Furthermore, we investigated the effect of NAC on the differentiation to myofibroblasts. High concentrations of NAC completely inhibited the TGF-β_1-stimulated α-SMA expression. These data suggested that NAC inhibited not only TGF-β_1 signaling [11] but also the TGF-β_1-mediated wound healing process and differentiation to myofibroblasts.

In the current paper, we confirmed the inhibitory effect of NAC on TGF-β_1-mediated physiological phenomena in vitro. TGF-β_1 signal transduction was completely blocked by NAC because NAC or DTT reduced TGF-β_1 and inhibited the binding to its receptor as a previous paper showed [11]. An other previous study showed that the dimeric form of TGF-β_1 disappeared after incubation with thiols by using mass spectroscopy [18]. Therefore, we need careful evaluation of the effects of reducing agents such as NAC or glutathione.

Fibronectin, a multifunctional glycoprotein involved in tissue remodeling, is a chemoattractant for lung fibroblasts [19] and can be released in increased amounts by fibroblasts [20] and epithelial cells [21] in response to a variety of cytokines. TGF-β_1 is the strongest stimulator of fibronectin release from fibroblasts. Because the excessive production of extracellular matrix is related to tissue remodeling, it appears that NAC can inhibit the TGF-β_1-induced fibronectin production to block abnormal tissue remodeling.

VEGF is a multifunctional growth factor. It was initially characterized as a factor that increases endothelial permeability and induces endothelial cell growth. It is not only essential for the

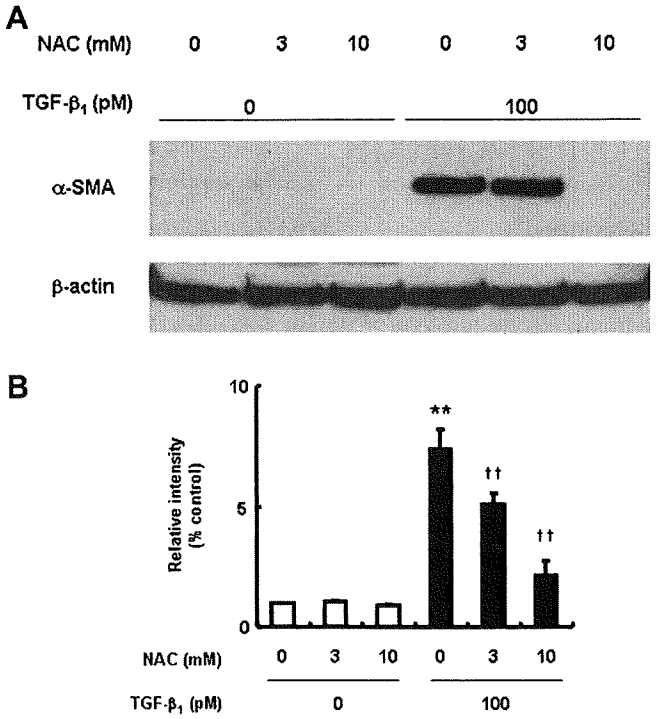

Fig. 3. Effect of NAC on the TGF-β_1-stimulated α-SMA expression. Fibroblasts were treated with or without various concentrations of NAC for 2 h prior to treatment with or without TGF-β_1. After 48 h, the cells were harvested and whole cell lysates were separated by SDS-PAGE. Expression of α-SMA was evaluated by western blotting (A). Intensity of bands detected by western blotting was quantified using NIH image (B). All values are mean ± SEM for three separate experiments. $^{**}p < 0.01$; compared with the values of control. $^{++}p < 0.01$; compared with the values of TGF-β_1 treated group.

normal development of blood vessels in the embryo, but it is also required for the survival of endothelial cells as well as for angiogenesis [22]. We have recently reported that TGF-β_1-enhanced VEGF production via smad3 which is phosphorylated by the activated TGF-β_1 receptor [23]. In the present study, NAC abolished the TGF-β_1-enhanced VEGF production because NAC completely blocked smad3 signal transduction (data not shown). Therefore, NAC may inhibit the TGF-β_1-induced excessive production of VEGF in pathological conditions.

NAC has been used as a potent antioxidant in in vivo studies. In an animal model, NAC could suppress bleomycin-induced lung fibrosis [10]. In a previous paper, high dose administration of NAC with low dose steroids to patients with IPF significantly improved lung function [24]. Although the pathogenesis of IPF is not well understood, TGF-β_1 is a key molecule in the progression of IPF. Based on the current study, NAC may have an effect on lung fibrosis not only as an antioxidant but also a reducing agent for TGF-β_1 itself.

In summary, our data demonstrated that NAC inhibited the TGF-β_1-augmented collagen gel contraction, mediator production, and α-SMA expression in fibroblasts. Since NAC was reported to inactivate TGF-β_1 itself and inhibit the binding to its receptor, its effect on TGF-β_1-induced phenomena in vitro should be carefully evaluated. The effects of NAC on the TGF-β_1-mediated profibrotic change in vivo may be mediated through not only an antioxidant but also an inactivator of TGF-β_1.

Acknowledgement

The authors thank Mr. Brent Bell for reading the manuscript.

References

[1] Keane MP, Henson PM, Strierer RM. Inflammation, injury, and repair. In: Murray JF, Nadel JA, editors. Textbook of respiratory medicine. Philadelphia: W.B. Saunders Company; 2000. p. 495–p.538.
[2] Tiddens H, Siverman M, Bush A. The role of inflammation in airway disease: remodeling. Am J Respir Crit Care Med 2000;162:S7–10.
[3] Rennard SI. Inflammation and repair processes in chronic obstructive pulmonary disease. Am J Respir Crit Care Med 1999;160:S12–6.
[4] Selman M, Pardo A. The epithelial/fibroblastic pathway in the pathogenesis of idiopathic pulmonary fibrosis. Am J Respir Cell Mol Biol 2003;29:S93–7.
[5] Blobe GC, Schiemann WP, Lodish HF. Role of transforming growth factor beta in human disease. N Engl J Med 2000;342:1350–8.
[6] Kobayashi T, Liu X, Wen FQ, Kohyama T, Shen L, Wang XQ, et al. Smad3 mediates TGF-beta1-induced collagen gel contraction by human lung fibroblasts. Biochem Biophys Res Commun 2006;339:290–5.
[7] Finesmith TH, Broadley KN. Fibroblasts from wounds of different stages of repair vary in their ability to contract a collagen gel in response to growth factors. J Cell Physiol 1990;144:99–107.
[8] Cuzzocrea S, Mazzon E, Dugo L, Serraino I, Ciccolo A, Centrrino T, et al. Protective effects of n-acetylcysteine on lung injury and red blood cell modification induced by carrageenan in the rat. FASEB J 2001;15:1187–200.
[9] Liu RM, Liu Y, Forman HJ, Olman M, Tarpey MM. Glutathione regulates transforming growth factor-beta-stimulated collagen production in fibroblasts. Am J Physiol Lung Cell Mol Physiol 2004;286:L121–8.
[10] Hagiwara S, Ishii Y, Kitamura S. Aerosolized of N-acetylcysteine attenuates lung fibrosis induced by bleomycin in mice. Am J Respir Crit Care Med 2000;162:225–31.
[11] Meurer SK, Lahme B, Tihaa L, Weiskirchen R, Gressner AM. N-acetyl-L-cysteine suppresses TGF-β signaling at distinct molecular steps: the biological efficacy of a multifunctional, antifibrotic drug. Biochem Pharmacol 2005;70:1026–34.
[12] Elsdale T, Bard J. Collagen substrata for studies on cell behavior. J Cell Biol 1972;54:626–37.
[13] Mio T, Adachi Y, Romberger DJ, Ertl RF, Rennard SI. Regulation of fibroblast proliferation in three dimensional collagen gel matrix. In Vitro Cell Dev Biol 1996;32:427–33.
[14] Sugiura H, Liu X, Kobayashi T, Togo S, Ertl RF, Kawasaki S, et al. Reactive nitrogen species augment fibroblast-mediated collagen gel contraction, mediator production and chemotaxis. Am J Respir Cell Mol Biol 2006;34:592–9.
[15] Junn K, Lee KN, Ju HR, Han SH, Im JY, Kang HS, et al. Requirement of hydrogen peroxide generation in TGF-beta 1 signal transduction in human lung fibroblast cells: involvement of hydrogen peroxide and Ca2+ in TGF-beta 1-induced IL-6 expression. J Immunol 2000;165:2190–7.
[16] Asaga H, Kikuchi S, Yoshizato K. Collagen gel contraction by fibroblasts requires cellular fibronectin but not plasma fibronectin. Exp Cell Res 1991;193:167–74.
[17] Wen FQ, Liu X, Manda W, Terasaki Y, Kobayashi T, Abe S, et al. TH2 cytokine-enhanced and TGF-beta-enhanced vascular endothelial growth factor production by cultured human airway smooth muscle cells is attenuated by IFN-gamma and corticosteroids. J Allergy Clin Immunol 2003;111:1307–18.
[18] White AC, Maloney EK, Lee SL, Lanzillo JJ, Fanburg BL. Reduction of endothelial cell related TGF beta activity by thiols. Endothelium 1999;6:231–9.
[19] Rennard SI, Hunninghake GW, Bitterman PB, Crystal RG. Production of fibronectin by the human alveolar macrophage: mechanism for the recruitment of fibroblasts to sites of tissue injury in interstitial lung diseases. Proc Natl Acad Sci U S A 1981;78:7147–51.
[20] Yoshida M, Romberger DJ, Illig MG, Takizawa H, Sacco O, Spurzem JR, et al. Transforming growth factor-β stimulates the expression of desmosomal proteins in bronchial epithelial cells. Am J Respir Cell Mol Biol 1992;6:439–45.
[21] Wang H, Liu X, Umino R, Skold CM, Zhu Y, Kohyama T, et al. Cigarette smoke inhibits human bronchial epithelial cell repair processes. Am J Respir Cell Mol Biol 2001;25:772–9.
[22] Leung DW, Cachianes G, Kuang WJ, Goeddel DV, Ferrara N. Vascular endothelial growth factor is a secreted angiogenic mitogen. Science 1989;246:1306–9.
[23] Kobayashi T, Liu X, Wen FQ, Fang Q, Abe S, Wang X, et al. Smad3 mediates TGF-beta1 induction of VEGF production in lung fibroblasts. Biochem Biophys Res Commun 2005;327:393–8.
[24] Behr J, Maier K, Degenkolb B, Krombach F, Vogelmeier C. Antioxidative and clinical effects of high-dose N-acetylcysteine in fibrosing alveolitis. Adjunctive therapy to maintenance immunosuppression. Am J Respir Crit Care Med 1997;156:1897–901.

Eur Respir J 2009; 34: 1452–1460
DOI: 10.1183/09031936.00195808

3-Nitrotyrosine inhibits fibroblast-mediated collagen gel contraction and chemotaxis

H. Sugiura*, X. Liu#, T. Ichikawa*, M. Ichinose* and S.I. Rennard#

ABSTRACT: **Reactive nitrogen species induce tissue inflammation and nitrate tyrosine residues of various kinds of proteins. Recent studies have established that the free amino acid form of 3-nitrotyrosine induces cytotoxity and growth inhibition and alters the cellular function in cultured cells. The aim of this study was to evaluate whether 3-nitrotyrosine could affect tissue remodelling in fibroblasts. To accomplish this, human fetal lung fibroblasts (HFL-1) were used to assess the fibroblast-mediated contraction of floating gels and chemotaxis towards fibronectin. In addition, the ability of fibroblasts to release fibronectin, transforming growth factor (TGF)-β1, fibronectin and vascular endothelial growth factor (VEGF) was assessed. 3-Nitrotyrosine significantly inhibited gel contraction ($p<0.01$) compared with control and this inhibition was abolished by nitric oxide synthase (NOS) inhibitor. 3-Nitrotyrosine did not affect TGF-β1 and VEGF but significantly decreased fibronectin release ($p<0.01$) into the media. 3-Nitrotyrosine significantly inhibited chemotaxis towards fibronectin through suppression of $\alpha_5\beta_1$ integrin expression ($p<0.01$). NOS inhibitor also reversed 3-nitrotyrosine-inhibited chemotaxis ($p<0.01$). Finally, 3-nitrotyrosine enhanced the expression of the inducible type of NOS ($p<0.01$) and nitric oxide release ($p<0.01$) through nuclear factor-κB activation. These results suggest that the free amino acid form of 3-nitrotyrosine can affect the tissue repair process by modulating nitric oxide production.**

KEYWORDS: **Inducible nitric oxide synthase, nitric oxide, reactive nitrogen species, remodelling**

Excessively produced nitric oxide (NO) derived from the inducible type of NO synthase (iNOS) leads to the formation of reactive nitrogen species (RNS), including peroxynitrite and nitrogen dioxide, during inflammatory and immune processes in lung diseases [1]. These RNS are formed from NO and superoxide anions [2] or *via* the H_2O_2/peroxidase-dependent nitrite oxidation pathway [3]. Excessive RNS cause tissue injury, lipid peroxidation and nitration of tyrosine residues [1, 4]. A metabolite generally reflecting the *in vivo* production of RNS is the amino acid derivative 3-nitrotyrosine. The production of 3-nitrotyrosine has been observed in various inflammatory lung diseases, including chronic obstructive pulmonary disease [5, 6], bronchial asthma [5, 7], cystic fibrosis [8] and idiopathic pulmonary fibrosis [9].

3-Nitrotyrosine was thought to be a stable marker of RNS production [10]. However, recent studies have established that, in addition to serving as a "footprint" of RNS, the free amino acid form of 3-nitrotyrosine itself induces cytotoxity, growth inhibition and morphological changes, and consequently alters the cellular function in cultured cells [11–13]. These studies suggest that 3-nitrotyrosine may play a critical role in the tissue repair process. Indeed, its abundant production (1–120 μM) has been shown under several pathological conditions, including rheumatoid arthritis [14], liver transplantation [15], septic shock [16] and amyotrophic lateral sclerosis [17]. However, whether 3-nitrotyrosine can affect the tissue repair response remains unknown.

Inflammatory processes are frequently accompanied by alterations in the tissue structure. Such alterations may result from tissue damage due to active proteases or toxic moieties released by inflammatory cells. In addition, mediators released at inflammatory sites are capable of directly altering the cell function, leading to tissue repair and remodelling. In human lung fibroblasts, recent studies showed that cytokine stimulation is associated with iNOS gene expression [18]. Gaseous NO can also stimulate iNOS expression [19]. Furthermore, we have shown

AFFILIATIONS
*Third Dept of Internal Medicine, Wakayama Medical University School of Medicine, Wakayama, Japan.
#Pulmonary Medicine, Nebraska Medical Center, Omaha, NE, USA.

CORRESPONDENCE
H. Sugiura
Third Dept of Internal Medicine
Wakayama Medical University School of Medicine
811-1 Kimiidera
Wakayama
Wakayama 641-0012
Japan
E-mail: sugiura@wakayama-med.ac.jp

Received:
Dec 25 2008
Accepted after revision:
April 18 2009
First published online:
May 14 2009

European Respiratory Journal
Print ISSN 0903-1936
Online ISSN 1399-3003

This article has supplementary material accessible from www.erj.ersjournals.com

that cytokine-induced NO inhibited collagen gel contraction, which is a novel tissue repair model [20]. These studies suggest that iNOS expression can be stimulated in human lung fibroblasts and NO derived from iNOS may affect the tissue repair process. On the basis of these observations, we hypothesised that the free amino acid form of 3-nitrotyrosine can modulate iNOS expression in human lung fibroblasts and affect the tissue repair process.

The present study, therefore, was designed first to determine whether 3-nitrotyrosine could affect tissue remodelling through an effect on the human fetal lung fibroblast (HFL-1)-mediated contraction of collagen gels and chemotaxis towards chemoattractant. Next, we assessed whether 3-nitrotyrosine can modulate fibroblast release of fibronectin, transforming growth factor (TGF)-β1 and vascular endothelial growth factor (VEGF), which are thought to be critical mediators of tissue remodelling. Finally, we determined whether the effects of 3-nitrotyrosine were mediated through excessive production of NO derived from iNOS.

MATERIALS AND METHODS

Materials

Native type I collagen (rat tail tendon collagen (RTTC)) was extracted from rat tail tendons by a previously published method [21]. Briefly, tendons were excised from rat tails, and the tendon sheath and other connective tissues were removed carefully. Repeated washing with Tris-buffered saline (0.9% NaCl and 10 mM Tris, pH 7.5) was followed by dehydration and sterilisation with 50%, 75%, 95% and pure ethanol. Type I collagen was then extracted in 6 mM hydrochloric acid at 4°C. The collagen concentration was determined by weighing a lyophilised aliquot from each lot of collagen solution. Sodium dodecylsulfate-polyacrylamide gel electrophoresis (SDS-PAGE) consistently demonstrated no detectable proteins other than type I collagen.

Commercially available reagents were obtained as follows: 3-nitrotyrosine, indomethacin, N^G-mono-methyl-L-arginine acetate salt (L-NMMA), sodium nitroprusside (SNP), L-N^6-(1-iminoethyl) lysine (L-NIL), 3,3',5,5'-tetramethylebenzidine, lipopolysaccharide (LPS) and 3-(4,5-dimethylthiazol-2-yl)-2,5-diphenyltetrazolium bromide (MTT) were from Sigma (St Louis, MO, USA); caffeic acid phenethyl ester (CAPE) and nuclear factor (NF)-κB inhibitors were from Calbiochem (La Jolla, CA, USA); Dulbecco's modified Eagle medium (DMEM) and fetal calf serum (FCS) were from Invitrogen Life Technologies (Grand Island, NY, USA).

Cell culture

HFL-1 cells were obtained from the American Type Culture Collection (Rockville, MD, USA). The cells were cultured on tissue culture dishes (Falcon; Becton-Dickinson Labware, Lincoln Park, NJ, USA) with DMEM supplemented with 10% FCS, 100 μg·mL^{-1} penicillin, 250 μg·mL^{-1} streptomycin and 2.5 μg·mL^{-1} fungizone. Cells were cultured at 37°C in a humidified atmosphere of 5% CO_2 and passaged every 4–5 days at a 1:4 ratio. HFL-1 cells were used between the 14th and 18th passages. At 30% confluence, cells were treated with varying concentrations of 3-nitrotyrosine in DMEM containing 10% FCS for 48 h. Cells were then harvested for later assay.

Collagen gel contraction assay

Collagen gels were prepared as described previously [22, 23]. Briefly, RTTC, distilled water and 4 × concentrated DMEM were combined so that the final mixture resulted in 0.75 mg·mL^{-1} collagen, with a physiological ionic strength of 1 × DMEM and a pH of 7.4. Cells were plated in 100-mm dishes in DMEM containing 10% FCS and treated with or without various concentrations of 3-nitrotyrosine for 48 h. To investigate the effect of the NOS inhibitors on fibroblast-mediated gel contraction, L-NMMA or L-NIL was added to the culture media in monolayers with or without varying concentrations of 3-nitrotyrosine. The cells were trypsinised (trypsin-EDTA: 0.05% trypsin, 0.53 mM EDTA-4Na; GIBCO, Invitrogen) and suspended in serum-free DMEM. The cells were then mixed with the neutralised collagen solution so that the final cell density in the collagen solution was 3×10^5 cells·mL^{-1} and the final concentration of collagen was 0.75 mg·mL^{-1}. Aliquots (0.5 mL·well^{-1}) of the mixture of cells in collagen were cast into each well of 24-well tissue culture plates (Falcon) and allowed to gel. After gelation was completed, normally within 20 min at room temperature, the gels were gently released from the 24-well tissue culture plates and transferred into 60-mm tissue culture dishes (three gels in each dish) that contained 5 mL of freshly prepared serum-free DMEM with or without various concentrations of 3-nitrotyrosine. The gels were then incubated at 37°C in a 5% CO_2 atmosphere for 3 days. To investigate the effect of L-NMMA or L-NIL on fibroblast-mediated gel contraction, L-NMMA or L-NIL was added to the culture media after the gels were released. Gel contraction was quantified daily using an Optomax V image analyser (Optomax, Burlington, MA, USA). Data were expressed as percentages of the original gel size.

Measurement of fibronectin, TGF-β1 and VEGF by ELISA

Fibronectin, TGF-β1 and VEGF in the media of the monolayer culture were determined by ELISA according to a previous report [23].

Chemotaxis assay

Cell migration was assessed using the Boyden blindwell chamber (Neuroprobe Inc., Gaithersburg, MD, USA) as previously described [23, 24]. Briefly, 26 μL of serum-free DMEM containing human fibronectin (20 μg·mL^{-1}) was placed into the bottom wells. Polycarbonate membranes with 8-μm pores (Neuroprobe Inc.), which were pre-coated with 5 μg·mL^{-1} gelatin in 0.1% acetic acid, were used. The cells were pretreated with or without various concentrations of 3-nitrotyrosine for 48 h. To investigate the role of NOS, L-NMMA was added to the culture media with or without 3-nitrotyrosine. The cells grown to 75% confluence were rinsed, re-fed with serum-free DMEM and treated with various concentrations of 3-nitrotyrosine at 37°C in a humidified atmosphere of 5% CO_2. The cells were trypsinised and suspended in serum-free DMEM at a density of 1×10^6 cells·mL^{-1}. 50 mL of cell suspension treated with various concentrations of 3-nitrotyrosine in the presence or absence of L-NMMA were then added into each top well. The cells were allowed to migrate at 37°C in a 5% CO_2 atmosphere for 6 h. Cells that had not migrated were scraped off the upper surface of the membrane and the membranes were air dried. The cells were then stained with PROTOCOL (Fisher Scientific, Swedesboro, NJ, USA) and mounted on a glass microscope slide. Chemotaxis was assessed by counting the numbers of cells in five high-power fields.

Wells with serum-free DMEM were used as negative controls and those with chemoattractant alone were used as positive controls.

Western blotting

To investigate the effects of NF-κB activation on iNOS expression, cells were treated with or without various concentrations of CAPE 30 min prior to treatment with 3-nitrotyrosine. After treatment with various concentrations of 3-nitrotyrosine for 48 h in a monolayer culture, cells were washed with 4°C PBS and homogenised in cell lysis buffer (35 mM Tris-HCl, pH 7.4, 0.4 mM EGTA, 10 mM $MgCl_2$, 1 μM phenylmethylsulfonyl fluoride, 100 $\mu g \cdot mL^{-1}$ aprotinin and 1 $\mu g \cdot mL^{-1}$ leupeptin). Samples were solubilised in SDS-PAGE sample buffer. To investigate NF-κB translocation into the nucleus, cells were seeded in 60-mm dishes at a density of 1×10^5 cells$\cdot mL^{-1}$. At 90% confluence, the cells were treated with 10^{-4} M 3-nitrotyrosine. The cells were harvested at various time points. To obtain the nuclear and cytosolic fractions, a nuclear extraction kit (Active Motif, Carlsbad, CA, USA) was used according to the manufacturer's instructions. Equal amounts of protein were loaded and separated by electrophoresis on 12.5% SDS-PAGE gels. After electrophoresis, the separated proteins were transferred to a polyvinylidene difluoride membrane (Bio-Rad Laboratories, Hercules, CA, USA). Primary polyclonal antibodies against human iNOS (1:100 dilution; Santa Cruz Biotechnology, Inc., Santa Cruz, CA, USA) or $\alpha_5\beta_1$ integrin (1:1,000 dilution; Chemicon International, Inc., Temecula, CA, USA), or mouse monoclonal anti-NF-κB p65 antibody (1:200 dilution; Santa Cruz Biotechnology, Inc.) were used for detection. Bound antibodies were visualised using appropriate peroxidase-conjugated secondary antibodies and enhanced chemiluminescence (Amersham Biosciences, Little Chalfont, UK) with a Typhoon Scanner (Amersham Biosciences). The intensity of the detected band was quantified by NIH image.

Quantitative PCR

Fibroblasts were treated with or without 3-nitrotyrosine and were harvested at 12 h. Total RNA was eluted using an RNeasy mini kit (Qiagen Sciences, Valencia, CA, USA). cDNA was generated using reverse transcriptase. The primers for iNOS were designed as follows: forward CCCCACGCTGCATTGG; reverse CACGTGTCTGCAGATGTGTTCA. Gene expression was measured using assays on the above probe and primers and reactions were analysed by using the ABI 7000 Taqman® system (Applied Biosystems, Foster City, CA, USA).

Measurement of nitrite/nitrate

To evaluate nitrite/nitrate production in the monolayer culture, cells were seeded in 6-well tissue plates at a cell density of 1×10^5 cells$\cdot mL^{-1}$. The cells were treated with or without varying concentrations of 3-nitrotyrosine for 48 h and the supernatant was harvested. The concentration of nitrite/nitrate was determined by a Nitric oxide assay kit (Assay Designs, Inc., Ann Arbor, MI, USA).

MTT assay

For monitoring cell viability, the 3-nitrotyrosine-treated cells were incubated with MTT solution at a final concentration of 1 $mg \cdot mL^{-1}$ for 4 h at 37°C. After incubation, dimethyl sulfoxide was added into each well. The absorbance of each sample at 570 nm was determined by a spectrophotometer using a reference wavelength of 630 nm.

Statistical analysis

Data were expressed as mean±SEM. Multiple comparisons of experimental values among the groups were evaluated by one-way ANOVA followed by Bonferroni's *post hoc* test to test for multiple comparisons and the Mann–Whitney U-test for single comparisons. Probability values of <0.05 were considered significant.

RESULTS

At first, we examined the effect of 3-nitrotyrosine on the cell viability. 3-Nitrotyrosine did not affect the cell viability in either the collagen gel culture condition or the chemotaxis condition (see supplementary fig. 1).

To investigate the 3-nitrotyrosine modulation of collagen gels, cells cast in collagen gels were floated in media with various concentrations of 3-nitrotyrosine. 3-Nitrotyrosine significantly inhibited the gel contraction compared with control in a concentration-dependent manner (at 10^{-4} M, gel size was 81.0±0.4% *versus* 65.9±0.1% of initial size on day 3; $p<0.01$; fig. 1). The NOS inhibitor L-NMMA (10^{-4} M) completely abolished the inhibitory effect of 3-nitrotyrosine on gel contraction compared with the 3-nitrotyrosine-treated group (on day 3, gel size was 71.5±0.7% *versus* 88.6±1.2% of initial size; $p<0.01$; fig. 2a), while the cyclooxygenase inhibitor indomethacin (2×10^{-6} M) had no effect on the 3-nitrotyrosine-mediated inhibition of gel contraction (on day 3, gel size was 86.4±1.0% *versus* 88.6±1.2% of initial size; fig. 2b). To investigate whether iNOS was related to the L-NMMA-mediated effect, the effects of a specific iNOS inhibitor L-NIL on the 3-nitrotyrosine-mediated inhibition of gel contraction was assessed. As shown in figure 3, L-NIL significantly reversed the 3-nitrotyrosine-mediated inhibition of gel contraction in a concentration-dependent manner (at 10^{-5}–10^{-4} M; $p<0.01$). To investigate the role of iNOS in the tissue repair, we treated the cells with LPS to stimulate the iNOS expression. LPS significantly augmented iNOS expression ($p<0.01$; supplementary fig. 2a). LPS significantly attenuated fibronectin release in the media compared with control (4,217±464 *versus* 8,131±585 ng$\cdot$culture^{-1}; $p<0.01$; supplementary fig. 2b). L-NIL significantly restored the LPS-attenuated fibronectin release (6,750±391 *versus* 4,217±464 ng$\cdot$culture^{-1}; $p<0.01$; supplementary fig. 2b).

It is known that fibronectin and TGF-β1 are involved in tissue repair and are able to enhance collagen gel contraction by human lung fibroblasts. VEGF is believed to contribute to vascular cell proliferation and may be a mediator of tissue repair and remodelling. To determine whether 3-nitrotyrosine could contribute to the release of these mediators, the release of these three mediators in the monolayer culture was evaluated. 3-Nitrotyrosine (10^{-5}–10^{-4} M) significantly decreased fibronectin release in the monolayer culture ($p<0.01$; fig. 4a), while it did not affect the release of TGF-β1 (fig. 4b) and VEGF (fig. 4c) in the monolayer culture.

Because fibroblast migration from neighbouring connective tissue into sites of inflammation plays an important role in tissue repair in response to injury, we assessed the effect of

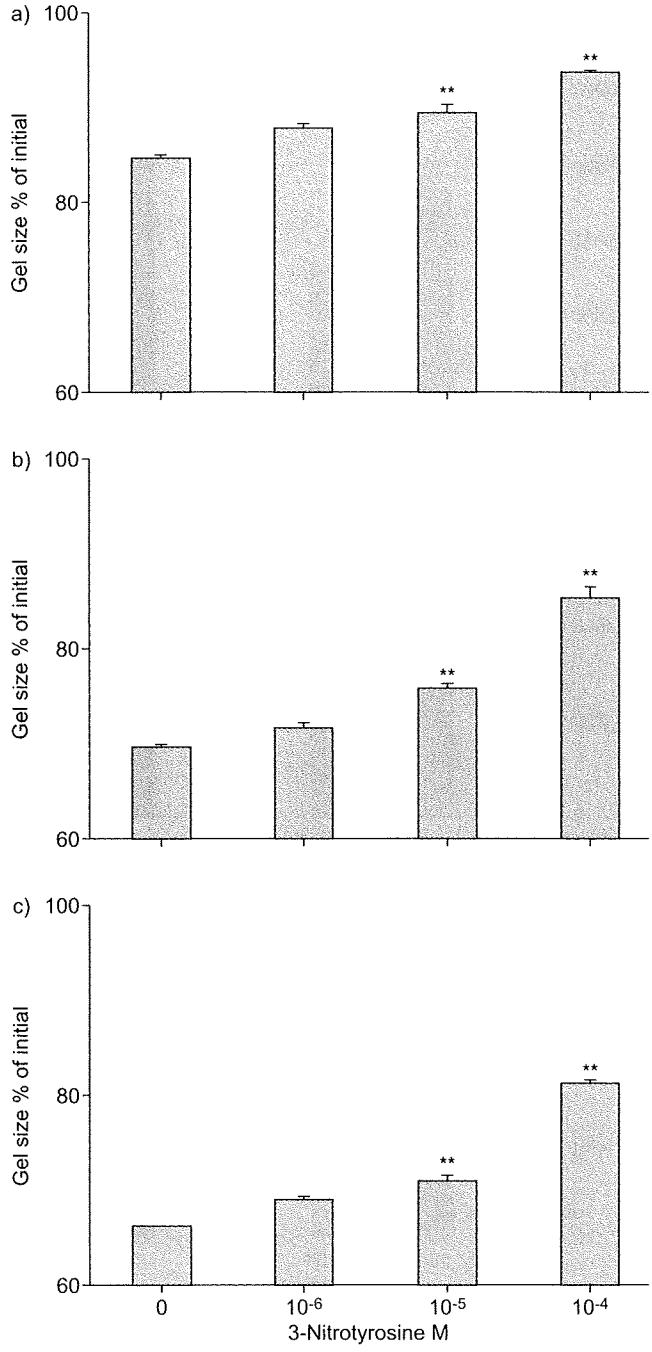

FIGURE 1. Effect of 3-nitrotyrsoine on collagen gel contraction by human fetal lung fibroblasts. Gel size was measured on a) day 1, b) day 2 and c) day 3. All values are mean±SEM for four separate experiments, each performed in triplicate. **: $p<0.01$ compared with control.

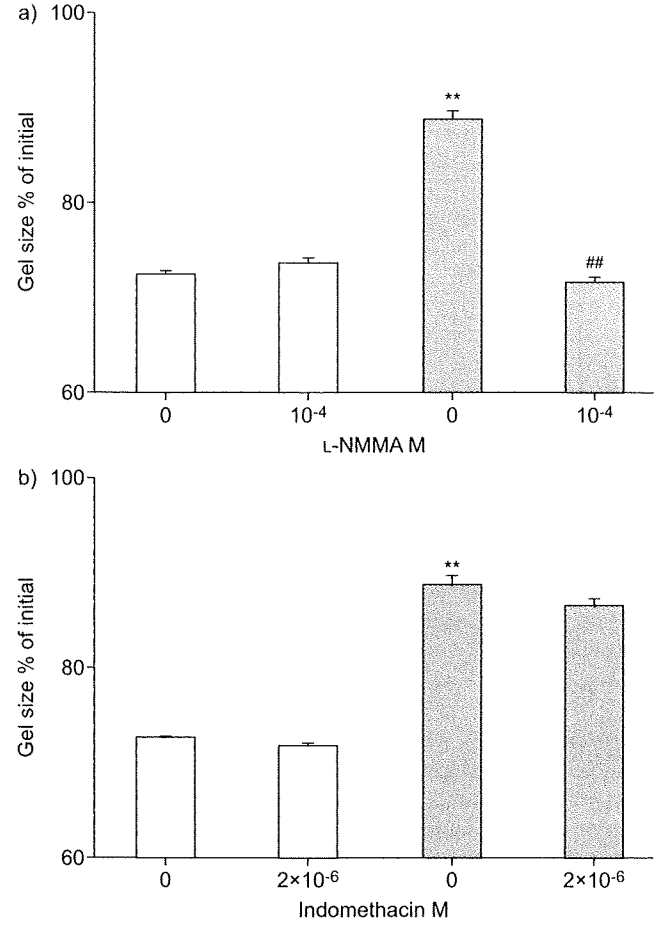

FIGURE 2. Effect of N^G-mono-methyl-L-arginine acetate salt (L-NMMA) and indomethacin on 3-nitrotyrosine-inhibited collagen gel contraction by human fetal lung fibroblasts. Fibroblasts were cast into collagen gels and maintained in floating culture in medium with (▨) or without (□) 3-nitrotyrosine at 10^{-4} M in the presence or absence of a) the nitric oxide synthase inhibitor L-NMMA or b) the cyclooxygenase inhibitor indomethacin. All values are mean±SEM for four separate experiments, each performed in triplicate. **: $p<0.01$ compared with control; ##: $p<0.01$ compared with 3-nitrotyrosine-treated group.

3-nitrotyrosine on HFL-1 chemotaxis. Using fibronectin (20 $\mu g \cdot mL^{-1}$) as the chemoattractant, 3-nitrotyrosine significantly inhibited fibroblast chemotaxis compared with control in a concentration-dependent manner (at 10^{-4} M, 248±24 cells in five high power fields (HPF) *versus* 95.0±14 cells in five HPF; $p<0.01$; fig. 5a). The NOS inhibitor L-NMMA (10^{-4} M) completely abolished the 3-nitrotyrosine-mediated inhibition of chemotaxis towards fibronectin ($p<0.01$; fig. 5a). We also investigated the effect of NO on fibroblast-mediated chemotaxis. The NO donor SNP inhibited the chemotaxis in a concentration-dependent manner (at 10^{-3} M, 223±14 cells in five HPF *versus* 108±9.8 cells in five HPF; $p<0.01$; fig. 5b). To explore the possible mechanism of inhibition of chemotaxis by 3-nitrotyrosine, we investigated the effect of nitrotyrosine on the expression of $\alpha_5\beta_1$ integrin, which is a receptor for fibronectin. As shown in figure 5c, 10^{-4} M 3-nitrotyrosine decreased the expression of $\alpha_5\beta_1$ integrin (both $p<0.05$).

To clarify which mechanisms are related to the 3-nitrotyrosine-augmented iNOS expression, we investigated the effect of 3-nitrotyrosine on NF-κB activation, which is thought to be the most important pathway in the regulation of iNOS expression. Fibroblasts were incubated with 3-nitrotyrosine and examined for the translocation of NF-κB p65 into the nucleus. There was no significant change in the translocation of NF-κB into the nucleus from 0 to 120 min without 3-nitrotyrosine treatment (*e.g.* at 0 min *versus* 60 min, 1.00±0.0 *versus* 1.04±0.15 relative intensity of

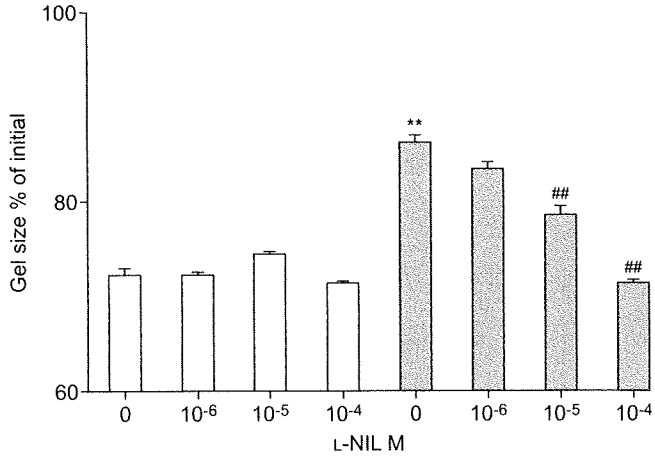

FIGURE 3. Effect of various concentrations of L-N^6-(1-iminoethyl)lysine (L-NIL) on 3-nitrotyrosine-mediated inhibition of gel contraction. Fibroblasts were maintained in floating culture in medium with (▒) or without (□) 3-nitrotyrosine at 10^{-4} M in the presence or absence of varying concentrations of L-NIL. All values are mean ± SEM for four separate experiments, each performed in triplicate. **: $p<0.01$ compared with control; ##: $p<0.01$ compared with vehicle-treated 3-nitrotyrosine-exposed group.

NF-κB/lamin A/C), whereas 10^{-4} M 3-nitrotyrosine significantly enhanced the translocation of NF-κB into the nucleus at 60 min as shown in figure 6a ($p<0.01$). Furthermore, a novel NF-κB inhibitor, CAPE, significantly suppressed the 3-nitrotyrosine-augmented iNOS expression (at 0.3–1.0 $\mu g \cdot mL^{-1}$ CAPE; $p<0.01$; fig. 6b). These results suggest that 3-nitrotyrosine stimulated NF-κB activation and augmented iNOS expression through NF-κB activation.

To clarify whether 3-nitrotyrosine augments the expression of iNOS, fibroblasts were incubated with 3-nitrotyrosine and examined for the expression of iNOS mRNA and protein. As shown in figure 7a and b, 10^{-4} M 3-nitrotyrosine significantly enhanced the expression of iNOS mRNA and protein ($p<0.01$). Furthermore, NO release in the media of the HFL-1 cell culture was investigated. 3-Nitrotyrosine significantly enhanced the release of NO in the media of the HFL-1 culture in a concentration-dependent manner (at 10^{-4} M; $p<0.01$; fig. 7c).

Because 3-nitrotyrosine is incorporated into α-tubulin in various types of cells and changes the cellular function, we investigated the incorporation of 3-nitrotyrosine into α-tubulin by western blotting. 3-Nitrotyrosine was not incorporated into α-tubulin in HFL-1 cells assessed by western blotting (supplementary fig. 3).

DISCUSSION

The present study demonstrated that the free amino acid form of 3-nitrotyrosine inhibits the fibroblast-mediated contraction of three-dimensional collagen gels and fibroblast chemotaxis towards fibronectin. 3-Nitrotyrosine also significantly decreased fibronectin release into the supernatant of the monolayer cultures. The NOS inhibitors L-NMMA and L-NIL recovered the 3-nitrotyrosine-inhibited gel contraction, mediator production and chemotaxis towards fibronectin. Furthermore, 3-nitrotyrosine enhanced the expression of iNOS protein through NF-κB activation and NO production. These results suggest that

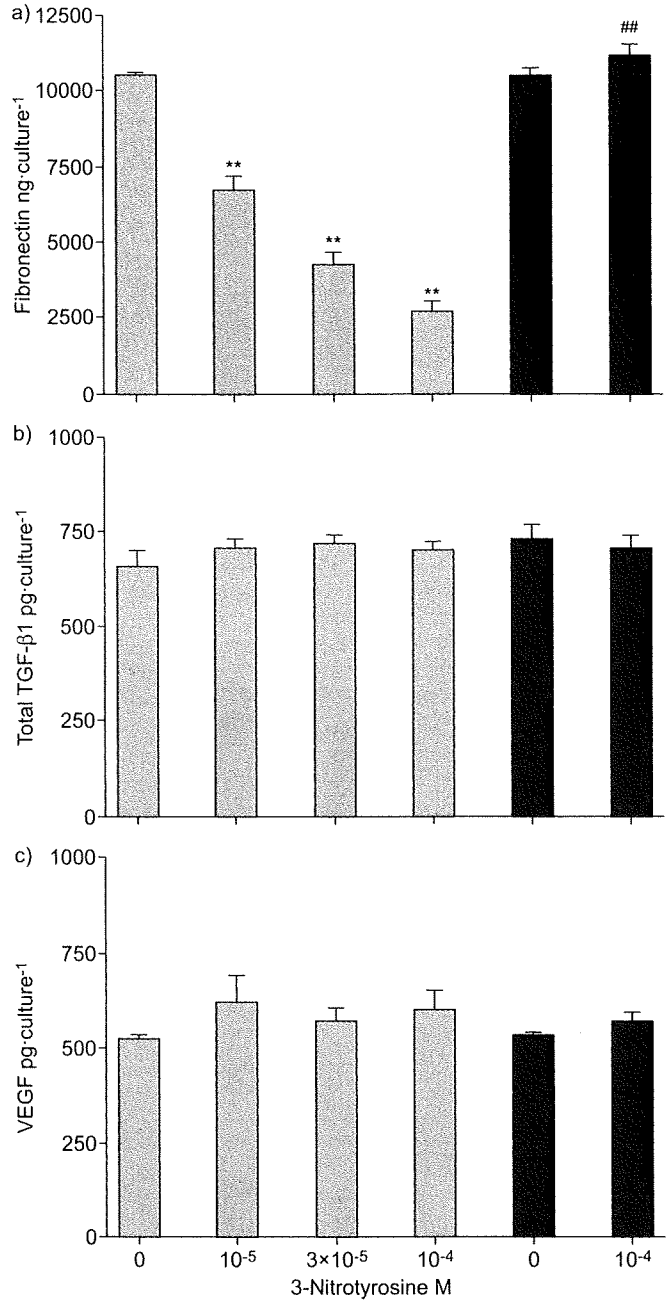

FIGURE 4. Effect of 3-nitrotyrosine on a) fibronectin, b) transforming growth factor (TGF)-β1 and c) vascular endothelial growth factor (VEGF) release. The effect of N^G-mono-methyl-L-arginine acetate salt at 10^{-4} M was also tested (■). Media were assayed by ELISA. All values are mean ± SEM for four separate experiments, each performed in duplicate. **: $p<0.01$ compared with control; ##: $p<0.01$ compared with vehicle-treated 3-nitrotyrosine-exposed (10^{-4} M) group.

3-nitrotyrosine can affect fibroblast-mediated repair processes and that the mechanism of this effect depends on the generation of NO.

3-Nitrotyrosine is a marker of nitration of the free amino acid form of tyrosine or tyrosine residues of proteins [4]. Recently, it has been reported that the free amino acid form of 3-nitrotyrosine is not only a marker of RNS, but also induces

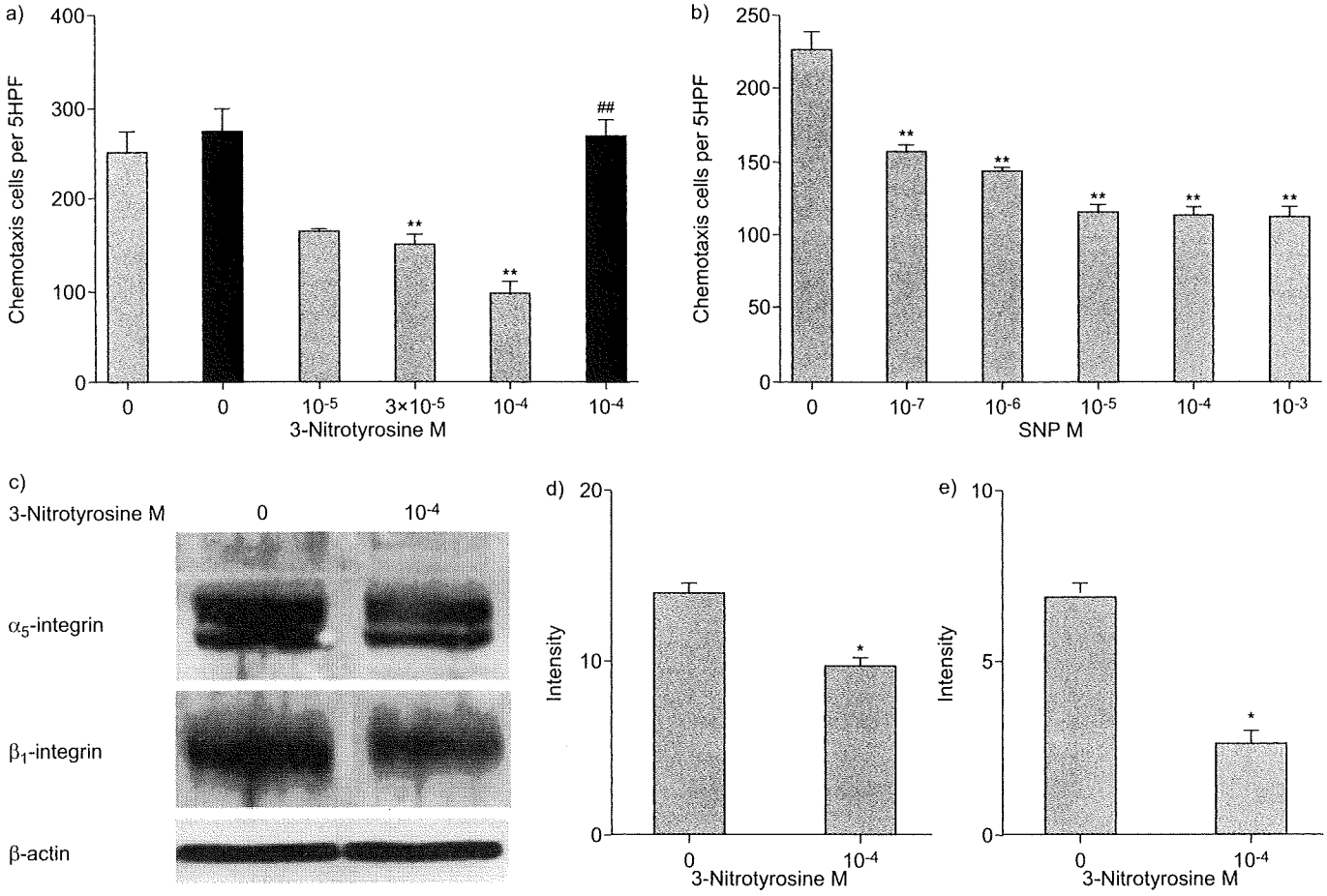

FIGURE 5. Effect of a) 3-nitrotyrosine or b) the nitric oxide donor sodium nitroprusside (SNP) on chemotaxis, and c) effect of 3-nitrotyrosine on expression of $\alpha_5\beta_1$ integrin in human fetal lung fibroblasts. Fibroblasts were exposed to various concentrations of a) 3-nitrotyrosine or b) SNP and assayed for chemotaxis towards fibronectin in the Boyden blindwell chemotaxis assay. The effect of N^G-mono-methyl-L-arginine acetate salt at 10^{-4} M was also tested (■). c) The treated cells were analysed by western blotting for the expression of $\alpha_5\beta_1$ integrin. Band intensity was quantified by NIH image for d) α_5-integrin and e) β_1-integrin. All values are mean±SEM for four separate experiments. *: $p<0.05$ compared with control; **: $p<0.01$ compared with control; ##: $p<0.01$ compared with 3-nitrotyrosine-treated (10^{-4} M) group.

cytotoxity, growth inhibition and morphological changes, and consequently alters the cellular function in cultured cells [11–13]. Our findings demonstrate that 3-nitrotyrosine leads to the decreased release of fibronectin that drives fibroblast-mediated repair responses. Fibronectin, a multifunctional glycoprotein involved in tissue remodelling, is a chemoattractant for lung fibroblasts [25] and can be released in increased amounts from fibroblasts [25] and epithelial cells [26, 27] in response to a variety of cytokines. According to a previous study, both the cellular type and plasma type of fibronectin enhanced collagen gel contraction [28]. In the present study, 3-nitrotyrosine reduced fibronectin production and NOS inhibitor reversed the 3-nitrotyrosine-reduced fibronectin production, suggesting that NO can reduce fibronectin production in human lung fibroblast.

RNS have a variety of biological effects, including tissue injury, lipid peroxidation and nitration of protein tyrosine residues. We have shown that RNS are excessively produced in the airways of asthmatics [5] and that endogenously produced RNS cause airway inflammation in late allergic response model [29]. Recently, we have shown that peroxynitrite, one of the RNS, stimulates fibroblasts. Peroxynitrite stimulates the differentiation of fibroblasts into myofibroblasts and extracellular matrix protein production *in vitro* [23, 30], suggesting that RNS induce fibroblast-mediated profibrotic responses. In the current study, free 3-nitrotyrosine caused the inhibition of tissue remodelling *in vitro*. 3-Nitrotyrosine produced by RNS may counteract the RNS-mediated profibrotic responses.

NO is synthesised in a variety of cell types by the enzyme NOS, which exists in constitutive and inducible isoforms [29]. It has been reported that inflammatory cytokines can induce iNOS in human pulmonary fibroblasts [18]. In the current study, 3-nitrotyrosine induced iNOS protein through NF-κB activation in human lung fibroblasts. 3-Nitrotyrosine can also stimulate NO production in fibroblasts. Furthermore, the NOS inhibitor L-NMMA and the iNOS inhibitor L-NIL diminished the 3-nitrotyrosine-induced inhibition of collagen gel contraction, chemotaxis and fibronectin production, suggesting that 3-nitrotyrosine might affect the tissue repair process through NO production derived from iNOS.

The regulation of fibroblast recruitment *in vivo* is likely to depend on both the chemotactic factors and inhibitors.

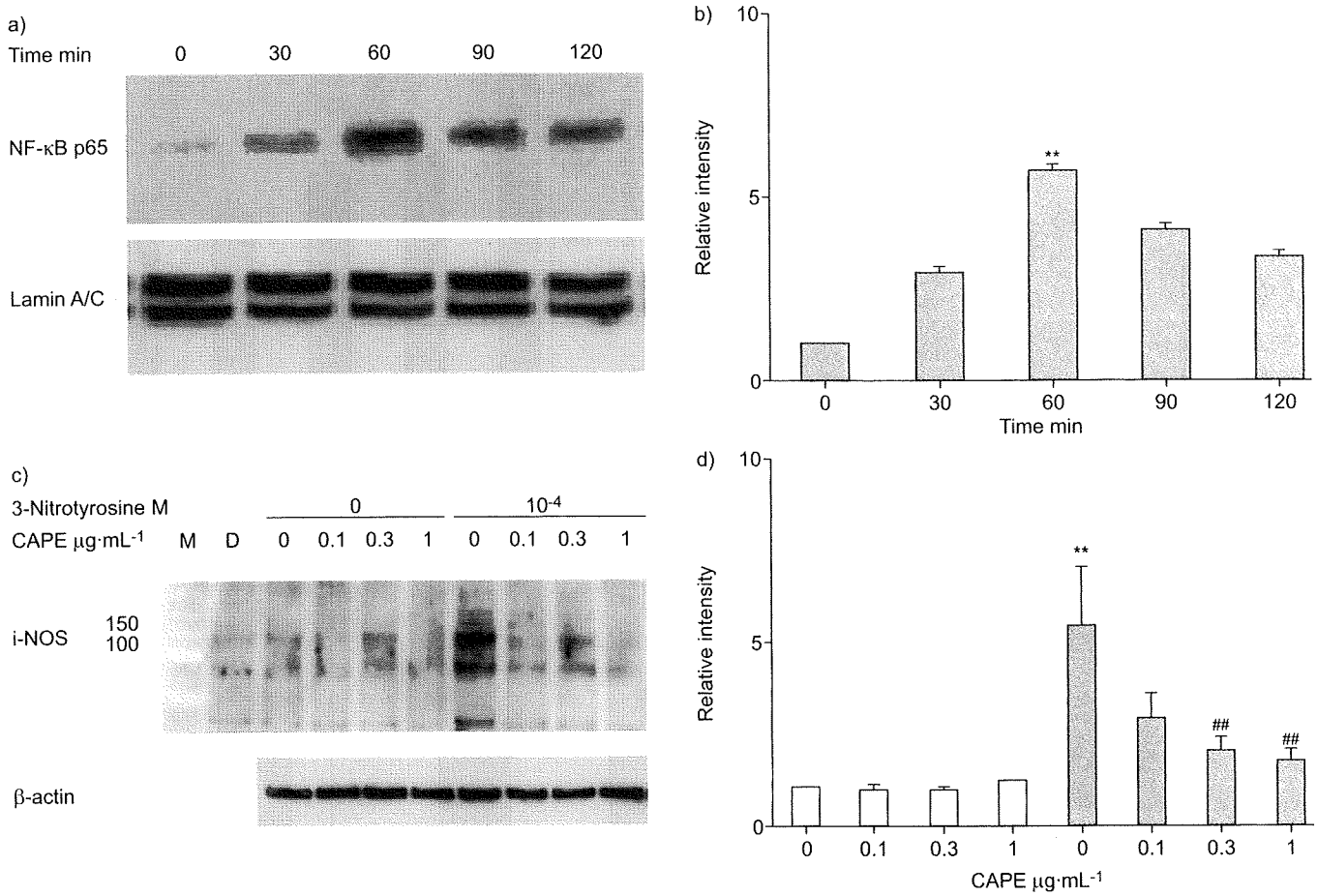

FIGURE 6. Effect of 3-nitrotyrosine on nuclear factor (NF)-κB p65 translocation into the nucleus and effect of an NF-κB inhibitor on the 3-nitrotyrosine-augmented inducible type nitric oxide synthase (iNOS) expression. a and b) Cells were treated with 10^{-4} M 3-nitrotyrosine and harvested at 0–120 min. The amount of NF-κB p65 translocated into the nucleus was assessed by western blotting. c and d) Cells were pretreated with the NF-κB inhibitor, caffeic acid phenethyl ester (CAPE), followed by treatment with (▨) or without (□) 3-nitrotyrosine at 10^{-4} M for 48 h. Cells were harvested and iNOS expression was assessed by western blotting. b and d) Band intensity was quantified by NIH image. M: molecular marker lane; D: the same amount of control protein was loaded to prevent "smiling". All values are mean±SEM for four separate experiments. **: $p<0.01$ compared with control; ##: $p<0.01$ compared with vehicle-treated 3-nitrotyrosine-exposed group.

Fibronectin can augment chemotactic activity in fibroblasts [25]. The current study demonstrated that 3-nitrotyrosine inhibited chemotaxis and NOS inhibitor abolished the 3-nitrotyrosine-induced inhibition of chemotaxis. Exogenously administrated NO also inhibited the fibroblast-mediated chemotaxis. Moreover, 3-nitrotyrosine can stimulate iNOS expression and NO production. Taken together, 3-nitrotyrosine inhibits chemotaxis through NO production. To explore the possible mechanism by which 3-nitrotyrosine inhibits fibroblast-mediated chemotaxis towards fibronectin, we investigated the effect of 3-nitrotyrosine on the expression of $\alpha_5\beta_1$ integrin, which is a receptor for fibronectin. In the present study, we found that 3-nitrotyrosine inhibited the expression of $\alpha_5\beta_1$ integrin. Therefore, 3-nitrotyrosine may inhibit chemotaxis through the suppression of $\alpha_5\beta_1$ integrin expression.

3-Nitrotyrosine could stimulate iNOS protein expression and NO production in the current study. Interestingly, 3-nitrotyrosine can stimulate NF-κB translocation into the nucleus. In general, NF-κB activation is a key process in the regulation of iNOS expression. To our knowledge, this is the first report showing that 3-nitrotyrosine stimulates NF-κB activation in lung fibroblasts. Although RNS are reported to stimulate NF-κB [30], nitrotyrosine derived from RNS may cause inflammation through NF-κB.

In the current study, we attempted to examine the role of NO derived from all types of NOS in the fibroblast function. We found that NO could attenuate the fibroblast function because a nonspecific NOS inhibitor, L-NMMA, restored the 3-nitrotyrosine-inhibited gel contraction (fig. 2a). Then, we found that 3-nitrotyrosine augmented iNOS expression through NF-κB activation. In the next step, we investigated the effects of NO derived from iNOS on the fibroblast function by means of a specific iNOS inhibitor, L-NIL. As we expected, the iNOS inhibitor significantly restored the 3-nitrotyrosine-inhibited gel contraction to the same degree as L-NMMA, as shown in figures 2a and 3, suggesting that NO derived from iNOS is a key mediator in the attenuation of the fibroblast function. Although we only showed that NO derived from iNOS could inhibit the gel contraction in the present study, these findings encourage us to speculate that L-NIL also may inhibit other fibroblast functions, including mediator production, chemotaxis and NO release.

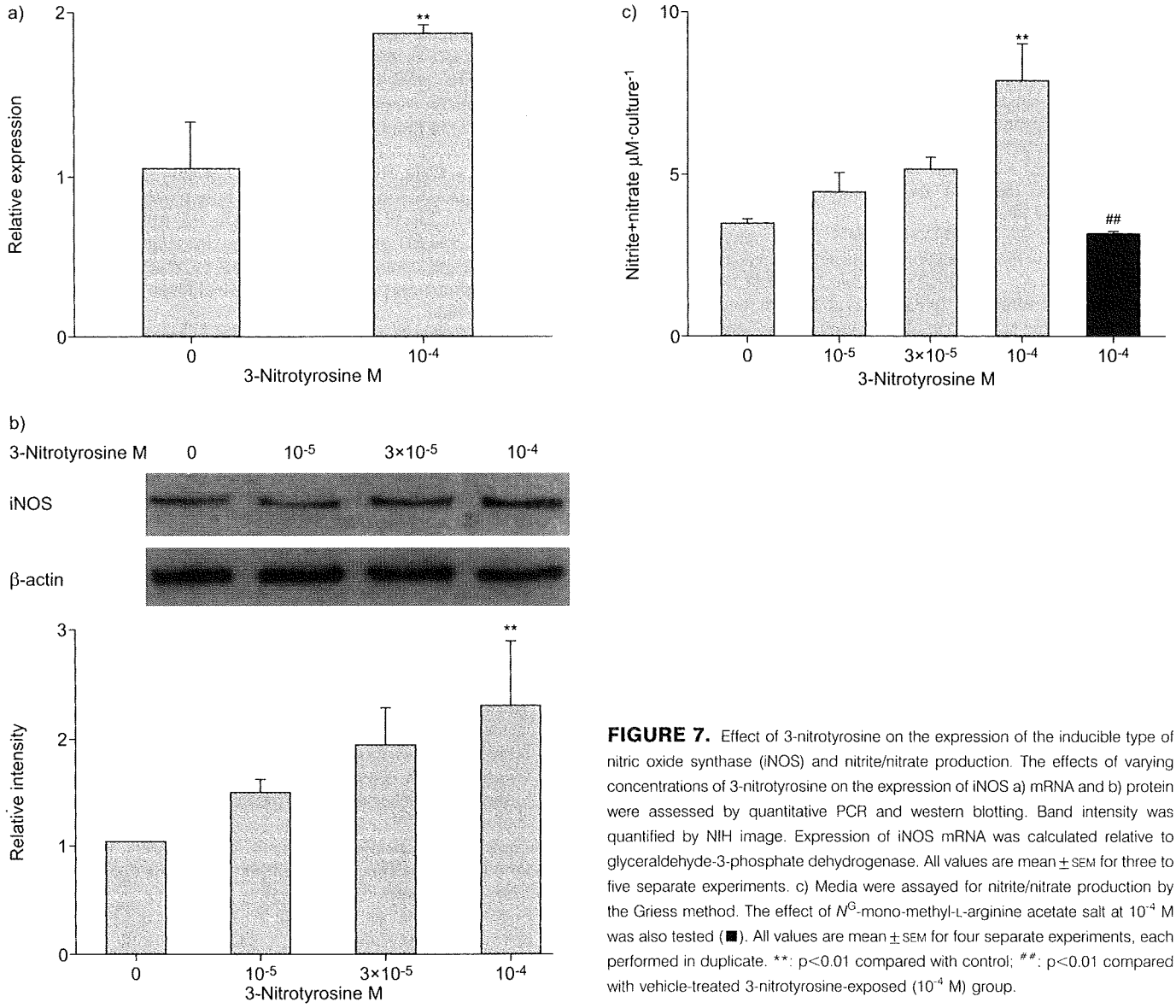

FIGURE 7. Effect of 3-nitrotyrosine on the expression of the inducible type of nitric oxide synthase (iNOS) and nitrite/nitrate production. The effects of varying concentrations of 3-nitrotyrosine on the expression of iNOS a) mRNA and b) protein were assessed by quantitative PCR and western blotting. Band intensity was quantified by NIH image. Expression of iNOS mRNA was calculated relative to glyceraldehyde-3-phosphate dehydrogenase. All values are mean±SEM for three to five separate experiments. c) Media were assayed for nitrite/nitrate production by the Griess method. The effect of N^G-mono-methyl-L-arginine acetate salt at 10^{-4} M was also tested (■). All values are mean±SEM for four separate experiments, each performed in duplicate. **: $p<0.01$ compared with control; ##: $p<0.01$ compared with vehicle-treated 3-nitrotyrosine-exposed (10^{-4} M) group.

It has been reported that 3-nitrotyrosine is incorporated into α-tubulin, induces cell morphology transformation and changes the cell function [13]. Therefore, we investigated whether 3-nirotyrosine attenuates the tissue repair because of the incorporation of 3-nitrotyrosine into α-tubulin. To clarify this, we investigated the incorporation of 3-nitrotyrosine into α-tubulin by western blotting. 3-Nitrotyrosine was not incorporated into the cells (supplementary fig. 3). However, we could not confirm whether the incorporation of 3-nitrotyrosine into α-tubulin is associated with the inhibition of tissue repair observed in the current study because of the lack of a specific tubulin tyrosine ligase inhibitor. The findings that 3-nitrotyrosine is not incorporated into the cells and that NOS inhibitors inhibited the 3-nitrotyrosine-mediated inhibition of tissue repair suggest that the 3-nitrotyrosine incorporation may have had little influence on our current findings.

In summary, our data demonstrate that 3-nitrotyrsine inhibited the fibroblast-mediated contraction of three-dimensional collagen gels, chemotaxis and fibronectin production. 3-Nitrotyrosine also augmented iNOS protein expression through NF-κB activation and the release of NO. These effects of 3-nitrotyrosine were significantly blocked by NOS inhibitor. These results suggest that the free amino acid form of 3-nitrotyrosine can affect the tissue repair process by modulating NO production.

STATEMENT OF INTEREST

A statement of interest for S.I. Rennard can be found at www.erj.ersjournals.com/misc/statements.dtl

ACKNOWLEDGEMENTS

The authors thank B. Bell (Division of Respiratory and Infectious Diseases, Tohoku University Graduate School of Medicine, Sendai, Japan) for reading the manuscript.

REFERENCES

1 van der Vliet A, Eiserich JP, Shigenaga MK, *et al.* Reactive nitrogen species and tyrosine nitration in the respiratory tract: epiphenomena or a pathobiologic mechanism of disease? *Am J Respir Crit Care Med* 1999; 160: 1–9.

2 Beckman JS, Beckman TW, Chen J, *et al.* Apparent hydroxyl radical production by peroxynitrite: implications for endothelial injury from nitric oxide and superoxide. *Proc Natl Acad Sci USA* 1990; 87: 1620–1624.
3 Eiserich JP, Hristova M, Cross CE, *et al.* Formation of nitric oxide-derived inflammatory oxidants by myeloperoxidase in neutrophils. *Nature* 1998; 391: 393–397.
4 Beckman JS, Koppenol WH. Nitric oxide, superoxide, and peroxynitrite: the good, the bad, and ugly. *Am J Physiol* 1996; 271: C1424–C1437.
5 Ichinose M, Sugiura H, Yamagata S, *et al.* Increase in reactive nitrogen species production in chronic obstructive pulmonary disease airways. *Am J Respir Crit Care Med* 2000; 162: 701–706.
6 Sugiura H, Ichinose M, Tomaki M, *et al.* Quantitative assessment of protein-bound tyrosine nitration in airway secretions from patients with inflammatory airway disease. *Free Radic Res* 2004; 38: 49–57.
7 Saleh D, Ernst P, Lim S, *et al.* Increased formation of the potent oxidant peroxynitrite in the airways of asthmatic patients is associated with induction of nitric oxide synthase: effect of inhaled glucocorticoid. *FASEB J* 1998; 12: 929–937.
8 van der Vliet A, Nguyen MN, Shigenaga MK, *et al.* Myeloperoxidase and protein oxidation in cystic fibrosis. *Am J Physiol Lung Cell Mol Physiol* 2000; 279: L537–L546.
9 Saleh D, Barnes PJ, Giaid A. Increased production of the potent oxidant peroxynitrite in the lungs of patients with idiopathic pulmonary fibrosis. *Am J Respir Crit Care Med* 1997; 155: 1763–1769.
10 Ye YZ, Strong M, Huang ZQ, *et al.* Antibodies that recognize nitrotyrosine. *Methods Enzymol* 1996; 269: 201–209.
11 Riccardi VM, Maragos VA. The pathophysiology of neurofibromatosis. I. Resistance *in vitro* to 3-nitrotyrosine as an expression of the mutation. *In Vitro* 1980; 16: 706–714.
12 MacLean SJ, Huber RE. The effects of DL-p-fluorophenylalanine and L-3-nitrotyrosine on the growth and biochemistry of the Taper liver tumor. *Cancer Res* 1971; 31: 1669–1672.
13 Eiserich JP, Estevez AG, Bamberg TV, *et al.* Microtubule dysfunction by posttranslational nitrotyrosination of α-tubulin: a nitric oxide-dependent mechanism of cellular injury. *Proc Natl Acad Sci USA* 1999; 96: 6365–6370.
14 Kaur H, Halliwell B. Evidence for nitric oxide-mediated oxidative damage in chronic inflammation. Nitrotyrosine in serum and synovial fluid from rheumatoid patients. *FEBS Lett* 1994; 350: 9–12.
15 Skinner KA, Crow JP, Skinner HB, *et al.* Free and protein-associated nitrotyrosine formation following rat liver preservation and transplantation. *Arch Biochem Biophys* 1997; 342: 282–288.
16 Fukuyama N, Takebayashi Y, Hida M, *et al.* Clinical evidence of peroxynitrite formation in chronic renal failure patients with septic shock. *Free Radic Biol Med* 1997; 22: 771–774.
17 Beal MF, Ferrante RJ, Browne SE, *et al.* Increased 3-nitrotyrosine in both sporadic and familial amyotrophic lateral sclerosis. *Ann Neurol* 1997; 42: 644–654.
18 Romanska HM, Polak JM, Coleman RA, *et al.* iNOS gene upregulation is associated with the early proliferative response of human lung fibroblasts to cytokine stimulation. *J Pathol* 2002; 197: 372–379.
19 Hsieh YS, Wang HC, Tseng TH, *et al.* Gaseous nitric oxide-induced 8-nitroguanine formation in human lung fibroblast cells and cell-free DNA. *Toxicol Appl Pharmacol* 2001; 172: 210–216.
20 Zhu YK, Liu XD, Skold MC, *et al.* Cytokine inhibition of fibroblast-induced gel contraction is mediated by PGE2 and NO acting through separate parallel pathways. *Am J Respir Cell Mol Biol* 2001; 25: 245–253.
21 Elsdale T, Bard J. Collagen substrata for studies on cell behavior. *J Cell Biol* 1972; 54: 626–637.
22 Mio T, Adachi Y, Romberger DJ, *et al.* Regulation of fibroblast proliferation in three dimensional collagen gel matrix. *In Vitro Cell Dev Biol* 1996; 32: 427–433.
23 Sugiura H, Liu X, Kobayashi T, *et al.* Reactive nitrogen species augment fibroblast-mediated collagen gel contraction, mediator production, and chemotaxis. *Am J Respir Cell Mol Biol* 2006; 34: 592–599.
24 Boyden S. The chemotactic effect of mixtures of antibody and antigen on polymorphonuclear leukocytes. *J Exp Med* 1962; 115: 453–466.
25 Rennard SI, Hunninghake GW, Bitterman PB, *et al.* Production of fibronectin by the human alveolar macrophage: mechanism for the recruitment of fibroblasts to sites of tissue injury in interstitial lung diseases. *Proc Natl Acad Sci USA* 1981; 78: 7147–7151.
26 Yoshida M, Romberger DJ, Illig MG, *et al.* Transforming growth factor-β stimulates the expression of desmosomal proteins in bronchial epithelial cells. *Am J Respir Cell Mol Biol* 1992; 6: 439–445.
27 Wang H, Liu X, Umino R, *et al.* Cigarette smoke inhibits human bronchial epithelial cell repair processes. *Am J Respir Cell Mol Biol* 2001; 25: 772–779.
28 Carnevali S, Nakamura Y, Mio T, *et al.* Cigarette smoke extract inhibits fibroblast-mediated collagen gel contraction. *Am J Physiol* 1998; 274: 591–598.
29 Sugiura H, Ichinose M, Oyake T, *et al.* Role of peroxynitrite in airway microvascular hyperpermeability during late allergic phase in guinea pigs. *Am J Respir Crit Care Med* 1999; 160: 663–671.
30 Ichikawa T, Sugiura H, Koarai A, *et al.* Peroxynitrite augments fibroblast-mediated tissue remodeling *via* myofibroblast differentiation. *Am J Physiol Lung Cell Mol Physiol* 2008; 295: L800–L808.

Respiratory Medicine (2010) 104, 228–236

available at www.sciencedirect.com

ScienceDirect

journal homepage: www.elsevier.com/locate/rmed

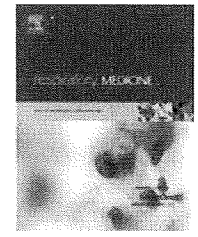

Tiotropium 5 μg via Respimat and 18 μg via HandiHaler; efficacy and safety in Japanese COPD patients

M. Ichinose [a,*], T. Fujimoto [b,d], Y. Fukuchi [c,e]

[a] *Wakayama Medical University, Wakayama, Japan*
[b] *Nippon Boehringer Ingelheim, Japan*
[c] *Juntendo University School of Medicine, Tokyo, Japan*

Received 19 August 2009; accepted 17 November 2009
Available online 6 December 2009

KEYWORDS
Bronchodilators;
COPD;
Inhalation devices;
Pharmacokinetics;
Tiotropium

Summary
Background and objectives: To compare the efficacy and safety of tiotropium inhaled via Respimat® Soft Mist Inhaler, a multidose propellant-free inhaler and HandiHaler®, a single-dose dry powder inhaler, in a phase 2 study of Japanese COPD patients.
Methods: Patients with $FEV_1 \leq 70\%$ predicted, $FEV_1/FVC \leq 70\%$ and a smoking history of >10 pack-years received tiotropium once daily via Respimat® (5 μg) and HandiHaler® (18 μg) for 4 weeks each in a randomised, double-blind, double-dummy, two-way crossover study. Lung function, adverse events, pharmacokinetics and safety were assessed.
Results: Of 184 patients screened, 134 were evaluable. The trough FEV_1 response on Day 29 showed Respimat® to be non-inferior to HandiHaler® (mean treatment difference, 0.008 L; 95% CI, −0.009 to +0.024 L; $p < 0.001$). Peak and average FEV_1 and FVC responses on Day 1 and Day 29 were very similar for the two treatments. Tiotropium plasma levels and excretion kinetics showed a similar profile of systemic exposure for the two formulations of tiotropium. Adverse events were reported by similar numbers of patients on each treatment, i.e. 27.9 and 30.6% in the Respimat® and HandiHaler® groups, respectively.
Conclusions: In Japanese patients with COPD, tiotropium Respimat® 5 μg and tiotropium HandiHaler® 18 μg showed a similar profile of efficacy, safety and pharmacokinetics.

* Corresponding author at: Third Department of Internal Medicine, Wakayama Medical University, 811-1, Kimiidera, Wakayama 641 8509, Japan. Tel.: +81 73 441 0619; fax: +81 73 447 2201.
E-mail address: masakazu@wakayama-med.ac.jp (M. Ichinose).
[d] Tsuyoshi Fujimoto, 2-1-1 Osaki, Shinagawa-ku, Tokyo 141 6017, Japan.
[e] Yoshinosuke Fukuchi, 2-9-8-901 Hongo, Bunkyo-ku, Tokyo 113 0033, Japan.

0954-6111/$ - see front matter © 2009 Elsevier Ltd. All rights reserved.
doi:10.1016/j.rmed.2009.11.011

Introduction

The anticholinergic agent tiotropium (Spiriva®) is a potent and long-acting bronchodilator whose clinical benefits when used chronically for the maintenance treatment of COPD have been established in several clinical studies.[1–4] When taken as a once daily inhalation, tiotropium improves lung function, reduces dyspnoea, reduces the incidence of exacerbations and improves health-related quality of life in patients with COPD.[5–10] It also reduces hyperinflation [11,12] and improves exercise tolerance.[12,13]

Tiotropium is the first long-acting anticholinergic approved for the treatment of COPD. It was first introduced in capsule form for inhalation via the HandiHaler®, a single-dose dry powder inhaler (DPI), and this form of tiotropium was given marketing approval in Japan in 2004. Recently, tiotropium has been introduced in a new inhaler device, the Respimat® Soft Mist Inhaler, a novel, multidose, propellant-free inhaler that delivers a fine particle fraction of over 65%.[14] The Respimat® inhaler generates a fine aerosol cloud that is generated over a longer period and moves more slowly than the aerosol from a pressurised metered-dose inhaler (pMDI). Because the aerosol cloud lasts 4–10 times longer than a pMDI aerosol,[15] the Respimat® inhaler offers the potential for easier co-ordination of inhalation with actuation of the inhaler. Deposition studies have shown that a higher proportion of the emitted dose from the Respimat® inhaler is delivered to the lungs than from a pMDI or from a multidose DPI.[16,17]

The results of a European phase II dose-ranging study on tiotropium in COPD patients showed that daily doses of 5–20 μg inhaled from the Respimat® inhaler were more effective than placebo in improving trough FEV_1 and other lung function measures after 3 weeks' treatment, and that steady-state urinary excretion of tiotropium with the 5 μg daily dosage from the Respimat® inhaler was similar to that with the 18 μg daily dosage from HandiHaler®.[18] Furthermore, in a pooled analysis of two crossover studies of identical design in American and European COPD patients, tiotropium Respimat® 5 μg was similar to tiotropium HandiHaler® 18 μg with respect to lung function improvement, pharmacokinetic profile and safety after 4 weeks' treatment.[19] On the basis of these results, a tiotropium dose of 5 μg from the Respimat® inhaler was considered to be comparable to an 18 μg dose from the HandiHaler® in American and European patients with COPD. The objective of the current study was to compare the same two treatments in Japanese COPD patients, to investigate whether the comparability also applies in this population. The effects of the two inhalers were compared using measurements of clinical efficacy, pharmacokinetic, tolerability and safety.

Methods

Study design

This phase 2 clinical trial used a randomised, double-blind, double-dummy, 2-way crossover design, and was conducted in 27 outpatient centres in Japan. The trial was carried out in compliance with principles laid down in the Declaration of Helsinki and in accordance with both the International Conference on Harmonisation (ICH) Harmonised Tripartite Guideline for GCP and Japanese GCP. The protocol and all amendments were approved by the local institutional review board, and all participants gave written informed consent. The trial is registered as NCT00292448 on ClinicalTrials.gov registry.

Patients

Japanese men or women were eligible for study entry if they were aged 40 years or older, had COPD (FEV_1 of no more than 70% predicted normal and ratio of FEV_1 to FVC of no more than 70%), and were current or ex-smokers (smoking history of >10 pack-years). Predicted normal FEV_1 values were calculated according to the standard formula for Japanese individuals.[20] To enter the second treatment period (Period 2), a patient's baseline FEV_1 reading at the start of that period had to be within ±15% of his or her reading at the start of the first treatment period. Patients were excluded if they had a history of asthma or allergic or atopic disease or, during the month before the screening visit, had received any specific treatment for such diseases (e.g. disodium cromoglycate, leukotriene antagonists, or antihistamines). Other exclusion criteria included a history of arrhythmias, or myocardial infarction in the previous year, or heart failure requiring hospital treatment in the previous 3 years, or treatment with beta-blockers during the month before the screening visit.

Treatments and crossover procedure

After the initial visit for patient screening, all participants entered a 4-week screening period during which they were instructed to practice inhalation from the Respimat® inhaler and HandiHaler®, using placebo versions of both test inhalers; patients also received instruction on correct preparation and inhalation technique for each inhaler. At the end of this period, patients meeting the entry criteria were randomly assigned in a 1:1 ratio to either regimen A or B for a 4-week period (Period 1):

Regimen A = tiotropium 5 μg inhaled via the Respimat® inhaler (two puffs of 2.5 μg each) plus placebo capsule inhaled via HandiHaler®, both given once daily in the morning.

Regimen B = placebo inhaled via the Respimat® inhaler (two puffs) plus tiotropium 18 μg capsule inhaled via HandiHaler®, both given once daily in the morning.

In both groups, the Respimat® inhaler was used first and HandiHaler® second (within 3 min of each other). After Period 1, patients entered a 4-week wash-out period (no study treatment), and then restarted study treatment for a further 4 weeks (Period 2), receiving whichever Regimen (A or B) they did not receive in the first period. For both treatment periods and the wash-out period, the allowable variance in duration was ±7 days.

The following concomitant medications were permitted at any time during the study provided the dosage was stable: inhaled short-acting beta-agonists (SABAs), which could also be used as rescue medication except on days when lung function tests were performed; oral or inhaled

corticosteroids; theophylline, and mucolytics. During the screening period and wash-out period only, the following additional medications were permitted (again at stable dosages only): inhaled long-acting beta-agonists (LABAs), oral and transdermal beta-agonists and inhaled short-acting anticholinergics.

Assessments

Pulmonary function tests (PFTs) were performed by spirometry at the screening visit to assess patients against screening criteria. Testing was repeated at the start and end (Day 1 and Day 29) of Periods 1 and 2 for efficacy measurements; on these occasions, tests were done 10 min before dosing of study medication, and 1, 2 and 3 h post-dose. At each time point, the highest FEV_1 and FVC values were recorded (from at least 3 attempts). The administration of other bronchodilators in the 24 h before the PFT was restricted to avoid confounding. For each patient, the baseline FEV_1 on Day 1 of Period 2 was required to be within ±15% of the baseline FEV_1 on Day 1 of Period 1. If this requirement was not met, the patient had up to two additional opportunities to comply, each within 7 days of the previous PFT.

To measure steady-state pharmacokinetics, blood and urine samples were taken at the end of both treatment periods (Day 29). Blood was taken pre-dose (no more than 1 h prior to dosing), then 10 min, 1.5 h and 4 h after dosing. For each patient, urine samples were combined into two separate collection periods, for the first 2 h after dosing and for the period 2–4 h after dosing. Plasma and urine levels of tiotropium were assayed by HPLC plus tandem mass spectrometry (HPLC–MS/MS) system, with a lower limit of quantification of 2.5 pg/ml in plasma samples and 10 pg/ml in urine samples. Steady-state kinetics were described by the parameters $AUC_{\tau,ss}$ and $Ae_{0-4,ss}$, i.e. the area under the tiotropium concentration-time curve over the dosing interval τ (24 h) and the amount of tiotropium in the urine in the 4 h after dosing.

Tolerability was assessed by adverse event monitoring from screening visit to 30 days after the last dose of study treatment. Any adverse event occurring after the first dose of a study treatment and up to 30 days after the last dose of the treatment was assigned to that treatment, as long as the next study treatment had not started.

At the screening visit and at the end of Periods 1 and 2, patients underwent physical examination and ECG, and had blood and urine sampled for haematology, urinalysis, and routine blood chemistry. Vital signs were measured at all visits (screening, and start and end of Periods 1 and 2).

Endpoints and statistical analysis

The Full Analysis Set (FAS), which consisted of the two treatment periods where baseline data and post-treatment data were available, was used for the analyses. The primary efficacy endpoint was the trough FEV_1 response, i.e. the difference between pre-dose FEV_1 on Day 1 of the treatment period and the pre-dose value on Day 29 of the same period. Using an analysis of covariance (ANCOVA) with terms for period, treatment and patient as fixed effects, and baseline FEV_1 as a covariate, the null hypothesis tested was that trough FEV_1 response with tiotropium Respimat® was inferior to that with tiotropium HandiHaler®. Assuming that the smallest clinically meaningful difference between treatments in this measure was 0.05 L, the null hypothesis could be rejected, i.e. tiotropium Respimat® would be non-inferior to tiotoprium HandiHaler®, if the lower 95% confidence limit (CL) for the difference between treatments (tiotropium Respimat® minus tiotropium HandiHaler®) was greater than −0.05 L.

Assuming a standard deviation in paired differences of trough FEV_1 of 0.12 L, 78 patients would need to complete the study to detect a difference in mean trough FEV_1 response between the two study treatments of at least 0.05 L with a significance level of 2.5% (one-sided) and 95% statistical power.

Secondary efficacy endpoints included the peak and average bronchodilator responses (measured as both FEV_1 and FVC) on Day 1 and Day 29. For both test days, peak response was the difference between the highest value recorded during the post-dose PFTs and the period baseline; average response was the area under the response-time curve during the first 3 h after dosing (AUC_{0-3h}). Estimates for peak and average responses were adjusted for patient, period and baseline value. Trough FVC response after 4 weeks, derived in the same way as trough FEV_1, was an additional efficacy endpoint. Analysis of all secondary efficacy endpoints was done using ANCOVA in the same way as for the primary endpoint, except that a two-tailed 95% confidence interval (CI) around the mean estimate was derived.

Analysis of tolerability, safety and pharmacokinetics data were done for all patients who had received at least one dose of study medication (the safety population).

Results

Patient disposition and screening characteristics

Of 184 patients enrolled at the screening visit, 157 met the criteria for entry to the study. In all, 134 patients completed the study (full analysis set), and 157 received at least one dose of study medication (safety population). A diagram of patient flow through each stage of the study is shown in Fig. 1.

At the screening visit, the great majority (98.1%) of COPD patients were men, and the mean age of the sample was 70.2 years (Table 1). Most were ex-smokers (77.1%). Although the average time since COPD diagnosis was 5.8 years, mean lung function measures at screening were an FEV_1 of 43.1% predicted normal and FEV_1/FVC ratio of 41.9%, and the majority of patients (66.9%) had severe or very severe COPD, i.e. Stage III or IV as defined by the Global Initiative for Chronic Obstructive Lung Disease (GOLD) guidelines.[21] These data, together with baseline values of FEV_1 and FVC for the two treatment groups, are shown in Table 1.

Efficacy

Primary endpoint

Graphs of change in mean FEV_1 in the 3 h after inhalation of tiotropium from each test inhaler show that on Day 1 and

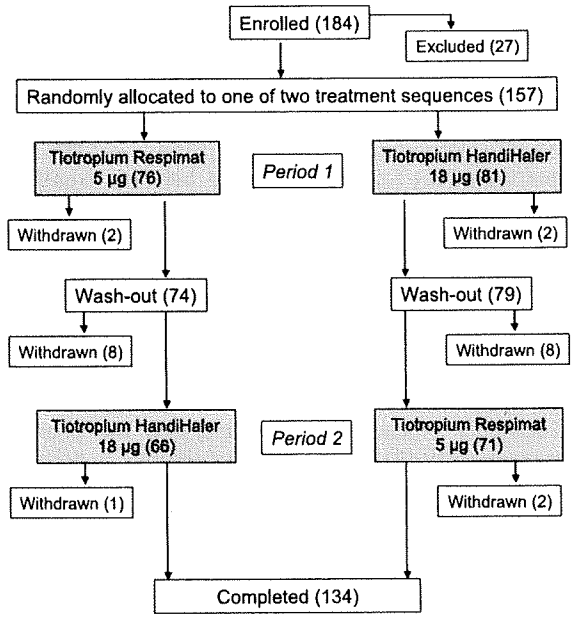

Figure 1 Patient flow through study.

Day 29, the bronchodilator responses to tiotropium were very similar for the Respimat® inhaler and HandiHaler® (Fig. 2a and b). Compared with the Day 1 baseline (pre-dose value), the mean pre-dose (trough) FEV_1 on Day 29 increased by 0.109 L and 0.101 L for the Respimat® inhaler and HandiHaler®, respectively. The mean difference in trough FEV_1 response between the inhalers was 0.008 L (95% CI, −0.009 to +0.024 L). As the lower CL was greater than −0.05 L, tiotropium Respimat® was non-inferior to tiotropium HandiHaler® ($p < 0.001$; Table 2).

In addition, the 95% CI for the mean estimated difference in trough FEV_1 between tiotropium Respimat® and tiotropium HandiHaler® lay entirely within the range of −0.05 L to +0.05 L, indicating very similar performance of the two inhalers according to this efficacy measure.

Secondary efficacy measures

The peak and average (AUC_{0-3h}) FEV_1 responses to tiotropium Respimat® were very similar to those to tiotropium HandiHaler® on Day 1 and Day 29, with no statistically significant differences between the two inhalers (Table 3).

The changes in FVC in the 3 h after inhalation of tiotropium from each test inhaler also show very similar responses for the two inhalers (Fig. 2c and d). On Day 29, the adjusted mean trough FVC value was higher that the pre-dose value on Day 1 by 0.213 L and 0.217 L for the Respimat® inhaler and HandiHaler® respectively; the difference between inhalers in trough FVC response (−0.004 L) was not significant ($p = 0.84$) (Table 4). For peak FVC responses and AUC_{0-3h} FVC responses on Day 1 and Day 29, there were also no significant differences between the two inhalers (Table 4).

Pharmacokinetics

Data from 153 patients was available for pharmacokinetic analysis. Steady-state plasma concentration-time profiles

Table 1 Characteristics of study participants at screening ($n = 157$ who took at least one dose of study medication) and spirometry measures at baseline (combined data for Periods 1 and 2; $n = 147$ for both treatments).

	Mean value (standard deviation)	Range
Values at screening visit		
Age, y	70.2 (7.5)	43–87
Men/women	154/3	–
Ex-smokers/ smokers, n	121/36	–
Smoking history, pack-years	60.4 (30.0)	20–150
Time since COPD diagnosis, y	5.8 (5.0)	0.1–38.0
FEV_1, L	1.171 (0.383)	0.35–2.21
FEV_1, % predicted	43.1 (13.3)	11–79
FVC, L	2.795 (0.646)	1.17–4.37
FEV_1/FVC ratio, %	41.9 (9.7)	19.8–69.7
GOLD stage, n (%):		
I	0 (0)	–
II	52 (33.1)	–
III	81 (51.6)	–
IV	24 (15.3)	–
Values at baseline		
FEV_1, L		
Tiotropium Respimat® 5 µg	1.072 (0.386)	0.37–2.11
Tiotropium HandiHaler® 18 µg	1.096 (0.381)	0.37–2.10
FVC, L		
Tiotropium Respimat® 5 µg	2.614 (0.621)	1.31–4.12
Tiotropium HandiHaler® 18 µg	2.662 (0.656)	1.21–4.40

for tiotropium were similar for the two inhalers (Fig. 3), and steady-state tiotropium plasma exposures ($AUC_{\tau,ss}$) were 94.4 and 89.6 pg h/ml (geometric mean values, $n = 128$) for the Respimat® inhaler and HandiHaler® respectively, giving an adjusted mean ratio for the Respimat® inhaler to HandiHaler® of 105.60%. For steady-state urinary excretion of unchanged tiotropium in the first 4 h after dosing, the respective values of $Ae_{0-4,ss}$ were 342 and 341 ng ($n = 128$), giving an adjusted mean ratio of 102.22%.

The 90% CLs of the adjusted mean ratios (Respimat®: HandiHaler®) were 98.00 and 113.78% for $AUC_{\tau,ss}$ and 92.50 and 112.96 for $Ae_{0-4,ss}$; both of these lay within the interval of 80–125%, thus meeting the criterion for therapeutic equivalence for orally administered drugs. For inhaled drugs, this finding indicates comparable systemic exposure with the two inhalers.

Tolerability and safety

Adverse events are summarised in Table 5. The number of adverse events reported during treatment with tiotropium

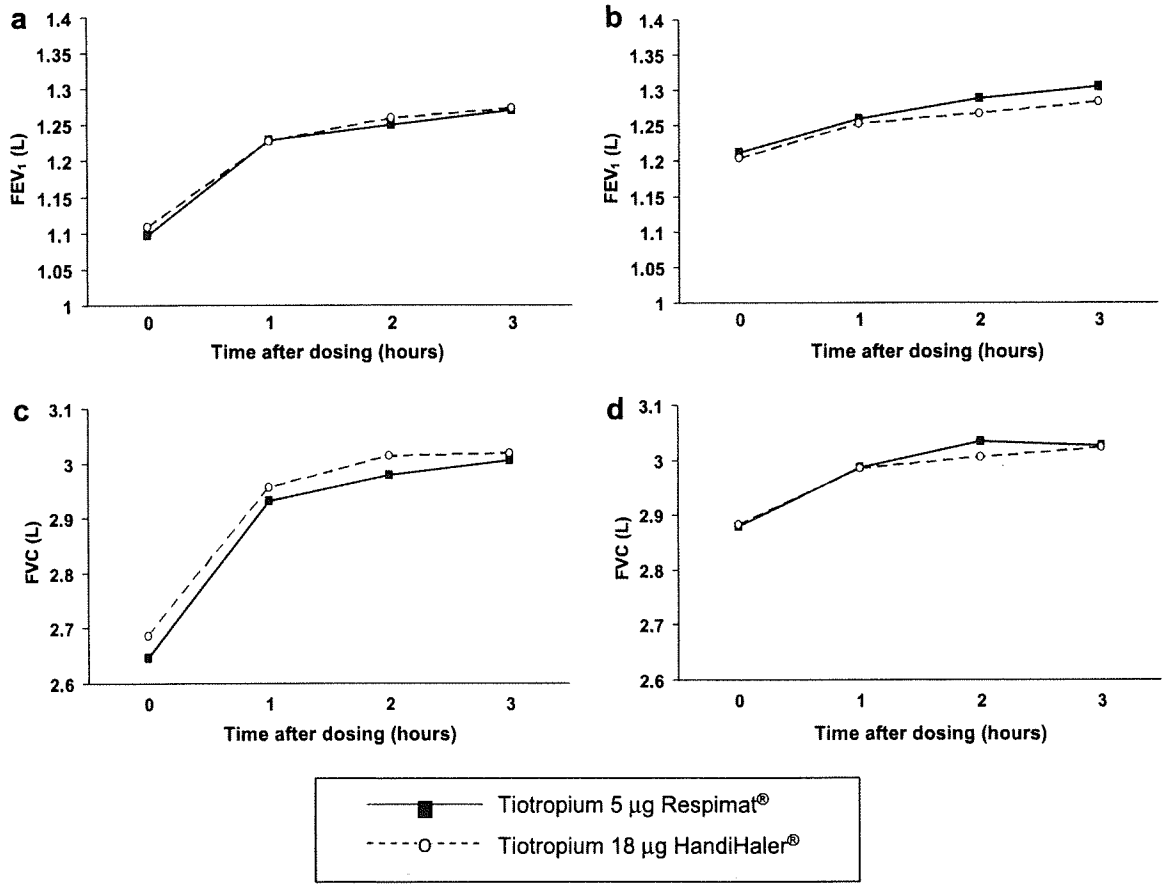

Figure 2 Changes in lung function parameters in the 3 h after dosing in full analysis set ($n = 134$): mean FEV_1 on Days 1 and 29 (a and b); mean FVC on Days 1 and 29 (c and d).

Respimat® (45; 30.6%) was similar to that with tiotropium HandiHaler® (41; 27.9%). The number of patients reporting adverse events considered by the investigator to be related to study treatment was low (4 [2.7%] and 8 [5.4%] patients during Respimat® and HandiHaler® treatment periods respectively). Three patients withdrew from the treatment phase of the study as a result of adverse events.

In all, 11 serious adverse events (SAEs) were reported by ten patients during the two treatment periods, none of which were considered to be related to study treatment. The 11 SAEs that occurred (five with Respimat® and six with HandiHaler®) were bacterial bronchitis, COPD exacerbation (4 events), haemorrhoids, oesophageal carcinoma, pneumonia,[2] pneumothorax and rheumatoid arthritis. No deaths occurred during the study.

Table 2 Non-inferiority analysis for trough FEV_1 increase (change in pre-dose FEV_1 from Day 1 to Day 29) in the full analysis set. Mean increases are adjusted for effects of patient, period and baseline FEV_1.

	N	Adjusted mean increase, L (SE)	Mean difference, L (SE)	95% CL	*p* value for non-inferiority[a]
Tiotropium Respimat® 5 µg	134	0.109 (0.006)	–	0.097, 0.120	–
Tiotropium HandiHaler® 18 µg	134	0.101 (0.006)	–	0.089, 0.113	–
Difference, Respimat minus HandiHaler®	134	–	0.008 (0.009)	−0.009, 0.024	$p < 0.001$

Abbreviations: CL, confidence limits; SE, standard error.
[a] One-sided ANCOVA for non-inferiority.

Table 3 Summary of peak and average (AUC_{0-3h}) FEV_1 responses on Day 1 and Day 29 in the full analysis set. Mean responses are adjusted for effects of patient, period and baseline FEV_1 on Day 1.

	Tiotropium Respimat® 5 μg ($n = 134$)	Tiotropium HandiHaler® 18 μg ($n = 134$)
Peak FEV_1, Day 1, L		
Adjusted mean response (95% CL)	0.186 (0.175, 0.196)	0.189 (0.179, 0.199)
Difference, Respimat® minus HandiHaler® (95% CL)	−0.003 (−0.018, 0.011)	
p value for difference between inhalers[a]	0.6481	
Peak FEV_1, Day 29, L		
Adjusted mean response (95% CL)	0.220 (0.208, 0.232)	0.205 (0.193, 0.217)
Difference, Respimat® minus HandiHaler® (95% CL)	0.015 (−0.002, 0.032)	
p value for difference between inhalers[a]	0.0925	
FEV_1 AUC_{0-3h}, Day 1, L		
Adjusted mean response (95% CL)	0.119 (0.111, 0.127)	0.122 (0.114, 0.130)
Difference, Respimat® minus HandiHaler® (95% CL)	−0.003 (−0.014, 0.009)	
p value for difference between inhalers[a]	0.6358	
FEV_1 AUC_{0-3h}, Day 29, L		
Adjusted mean response (95% CL)	0.166 (0.155, 0.177)	0.151 (0.140, 0.162)
Difference, Respimat® minus HandiHaler® (95% CL)	0.015 (−0.001, 0.030)	
p value for difference between inhalers[a]	0.0679	

Abbreviations: CL, confidence limits; SE, standard error.
[a] Two-sided ANCOVA.

In the listing of adverse events by preferred term, the most common events were nasopharyngitis (22 patients) and COPD exacerbation (10 patients). Dry mouth was reported by 5 patients. These and other common events, i.e. those occurring in 2% of more of patients on either inhaler, are listed in Table 5.

No clinically important drug-related changes were noted in the assessments of vital signs, ECG and laboratory test variables.

Discussion

In this study, we have shown that a daily tiotropium dose of 5 μg inhaled via the Respimat® inhaler was similar to a dose of 18 μg inhaled from HandiHaler® in terms of pulmonary function improvement and pharmacokinetics when both were given for a period of 4 weeks. As well as producing an acute bronchodilator effect after each daily dose, 4 weeks' treatment with tiotropium inhaled from both test inhalers was associated with an improvement in airway calibre as shown by an increase of roughly 100 ml in trough (pre-dose) FEV_1 over the period from Day 1 to Day 29. On the basis of this efficacy measure, tiotropium Respimat® was demonstrated to be non-inferior to tiotropium HandiHaler® at the doses studied in this trial ($p < 0.001$).

The similar clinical performance of tiotropium Respimat® 5 μg and tiotropium HandiHaler® 18 μg was confirmed by other spirometry measurements. The trough FVC at Day 29 was roughly 200 ml higher than the corresponding value on Day 1 with both inhalers and for this measure, as well as for peak and average (AUC_{0-3h}) FEV_1 and FVC results, differences between the two inhalers were not statistically significant. Our efficacy findings are in line with the results of a dose-ranging study that compared lung function after 3 weeks' treatment with tiotropium HandiHaler® 18 μg and a range of tiotropium doses from the Respimat® inhaler.[18] They also agree closely with a comparison done in European and North American COPD patients who received two different daily doses of tiotropium from the Respimat® inhaler (5 and 10 μg) and tiotropium 18 μg from HandiHaler®, each for 4 weeks in two crossover studies of identical design.[19] Pooled analysis of those studies demonstrated non-inferiority of tiotropium Respimat® 5 μg to tiotropium HandiHaler® 18 μg for the primary efficacy variable of trough FEV_1, and also showed trough FEV_1 responses to be statistically significantly higher with tiotropium Respimat® 5 μg, although the difference was small and of questionable clinical relevance.

Until now, no studies have been published on tiotropium pharmacokinetics in Japanese individuals (COPD patients or volunteers). Average tiotropium plasma concentrations and urinary excretion of tiotropium at steady-state (Day 29) were very similar for tiotropium Respimat® and tiotropium HandiHaler®. When adjusted mean ratios (Respimat®: HandiHaler®) were calculated for both parameters, the associated 90% CIs were within the interval of 80–125%, which meets the criterion for demonstrating therapeutic equivalence for orally administered drugs. The pooled analysis of the twin crossover studies mentioned above [19] also found that systemic exposures for tiotropium Respimat® 5 μg and tiotropium HandiHaler® 18 μg were similar, although urinary excretion of tiotropium was 26% higher in the tiotropium Respimat® 5 μg arm than in the tiotropium HandiHaler® 18 μg arm.

The number and type of adverse events reported in the current study did not indicate any difference in the tolerability of tiotropium Respimat® and tiotropium HandiHaler®, and safety assessments (vital signs, ECG and laboratory test values) did not suggest any adverse responses to either of the study treatments. These results are in line with those